Generalized Polarizabilities of the proton

Nikos Sparveris

PREN 2023 & μASTI

Mainz, June 26-30 2023

Temple University

Supported by the US DOE / NP award DE-SC0016577

Outline

Introduction to the GPs

Overview: Status & Challenges

Recent results (Jlab / MAMI)

Prospects (VCS-II @ Jlab, measuring w positrons, …)

Proton Polarizablities

Fundamental structure constants
(such as mass, size, shape, …)

Response of the nucleon to external EM field

Sensitive to the full excitation spectrum

Accessed experimentally through Compton Scattering

PDG

N BARYONS
($S = 0$, $I = 1/2$)
p, $N^+ = uud$; n, $N^0 = udd$

p $I(J^P) = \frac{1}{2}(\frac{1}{2}^+)$

Mass $m = 1.00727646681 \pm 0.00000000009$ u
Mass $m = 938.272046 \pm 0.000021$ MeV [a]
$|m_p - m_{\overline{p}}|/m_p < 7 \times 10^{-10}$, CL = 90% [b]
$|\frac{q_{\overline{p}}}{m_{\overline{p}}}|/(\frac{q_p}{m_p}) = 0.99999999991 \pm 0.00000000009$
$|q_p + q_{\overline{p}}|/e < 7 \times 10^{-10}$, CL = 90% [b]
$|q_p + q_e|/e < 1 \times 10^{-21}$ [c]
Magnetic moment $\mu = 2.792847356 \pm 0.000000023\ \mu_N$
$(\mu_p + \mu_{\overline{p}}) / \mu_p = (0 \pm 5) \times 10^{-6}$
Electric dipole moment $d < 0.54 \times 10^{-23}$ e cm
Electric polarizability $\alpha = (11.2 \pm 0.4) \times 10^{-4}$ fm^3
Magnetic polarizability $\beta = (2.5 \pm 0.4) \times 10^{-4}$ fm^3 (S = 1.2)
Charge radius, μp Lamb shift $= 0.84087 \pm 0.00039$ fm [d]
Charge radius, $e p$ CODATA value $= 0.8775 \pm 0.0051$ fm [d]
Magnetic radius $= 0.777 \pm 0.016$ fm
Mean life $\tau > 2.1 \times 10^{29}$ years, CL = 90% [e] ($p \to$ invisible mode)
Mean life $\tau > 10^{31}$ to 10^{33} years [e] (mode dependent)

Virtual Compton Scattering:

Virtuality of photon gives access to the GPs : $\alpha_E(Q^2)$ & $\beta_M(Q^2)$ (+ 4 spin GPs)
→ mapping out the spatial distribution of the polarization densities

Fourier transform of densities of electric charges and magnetization of a nucleon deformed by an applied EM field

Scalar Polarizablities

Response of internal structure to an applied EM field

Interaction of the EM field with the internal structure of the nucleon

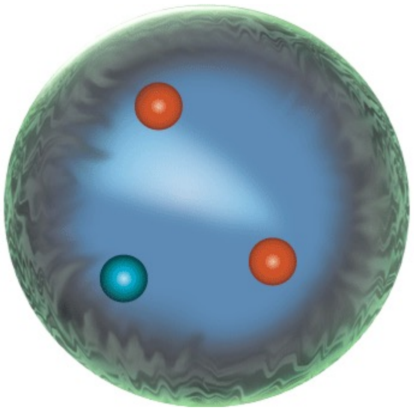

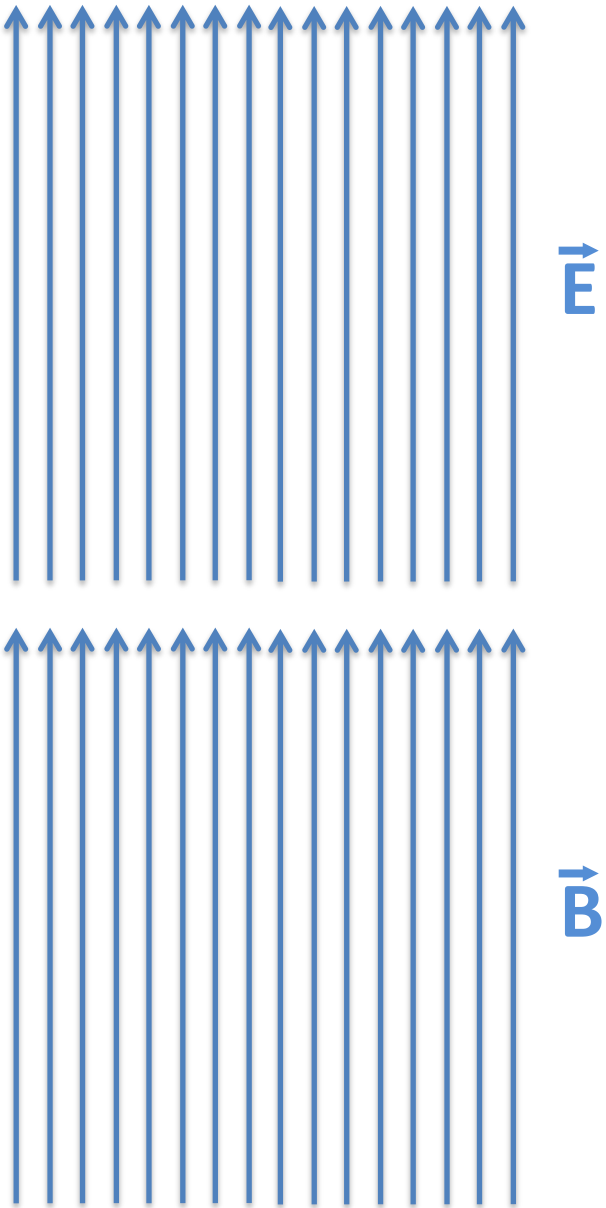

Scalar Polarizablities

Response of internal structure to an applied EM field

Interaction of the EM field with the internal structure of the nucleon

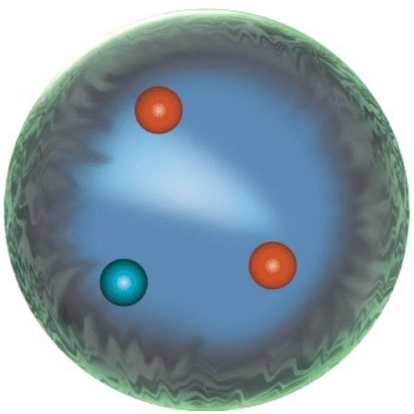

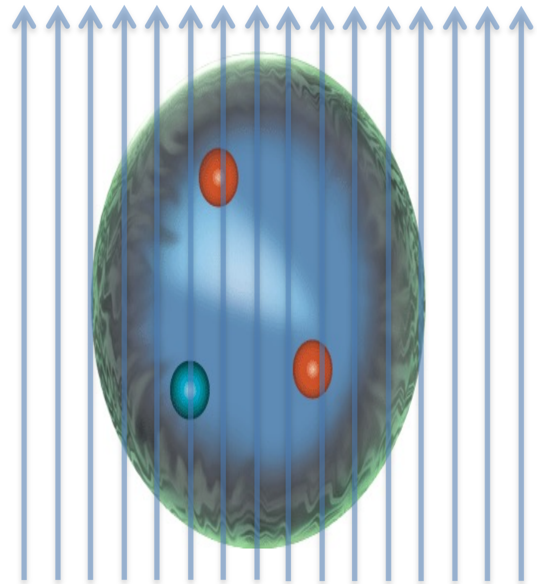

$\vec{E}$

"stretchability"

$\vec{d}_{E\ \mathrm{induced}} \sim \alpha\, \vec{E}$

External field deforms the charge distribution

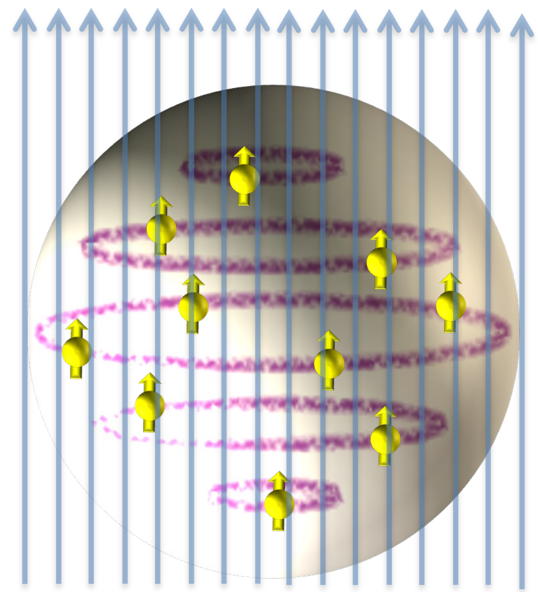

$\vec{B}$

"alignability"

$\vec{d}_{M\ \mathrm{induced}} \sim \beta\, \vec{B}$

$\beta_{para} > 0$

$\beta_{diam} < 0$

Paramagnetic: proton spin aligns with the external magnetic field

Diamagnetic: π-cloud induction produces field counter to the external perturbation

Virtual Compton Scattering

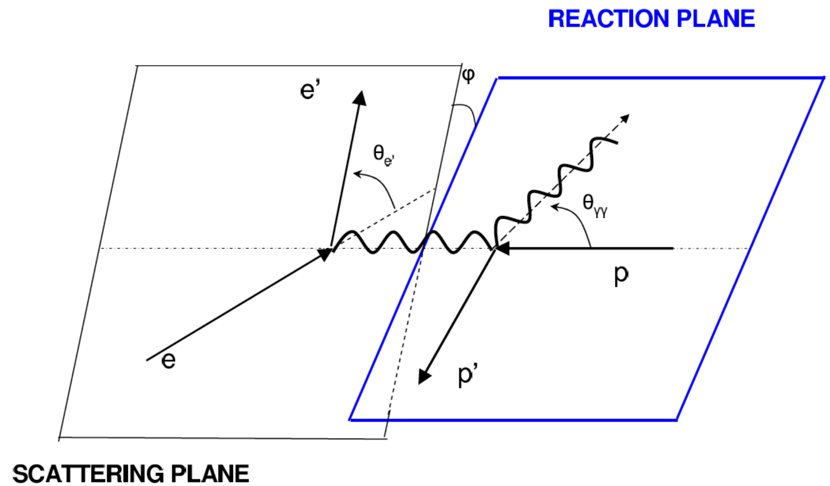

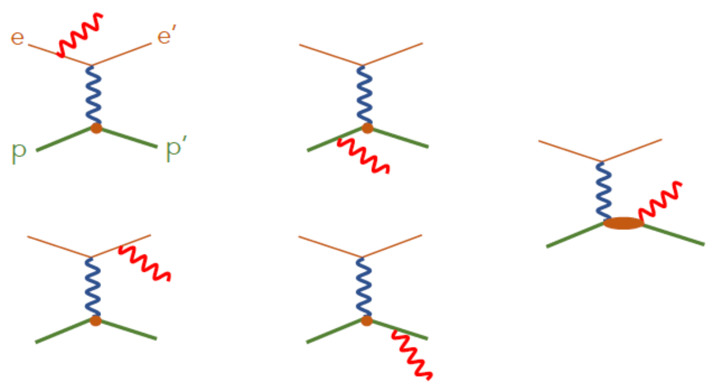

Bethe-Heitler Born VCS non-Born VCS

Elastic FFs

GPs

Virtual Compton Scattering

DR

valid below & above Pion threshold

Dispersive integrals for Non Born amplitudes

Spin GPs are fixed

Scalar GPs have an unconstrained part

Fit to the experimental cross sections at each Q^2

LEX

valid only below Pion threshold

Response functions

$$d^5\sigma = d^5\sigma^{BH+Born} + q'_{cm} \cdot \phi \cdot \Psi_0 + \mathcal{O}(q'^2_{cm})$$

$$\Psi_0 = v_1 \cdot (P_{LL} - \frac{1}{\epsilon} P_{TT}) + v_2 \cdot P_{LT}$$

Subtract the spin part

$$P_{TT} = [P_{TT\ spin}]$$

$$P_{LT} = -\frac{2M}{\alpha_{em}} \sqrt{\frac{q^2_{cm}}{Q^2}} \cdot G_E^p(Q^2) \cdot \beta_M(Q^2) + [P_{LT\ spin}]$$

utilize DR

scalar GPs α_E and β_M

Early Experiments

MIT-Bates @ Q^2=0.06 GeV^2

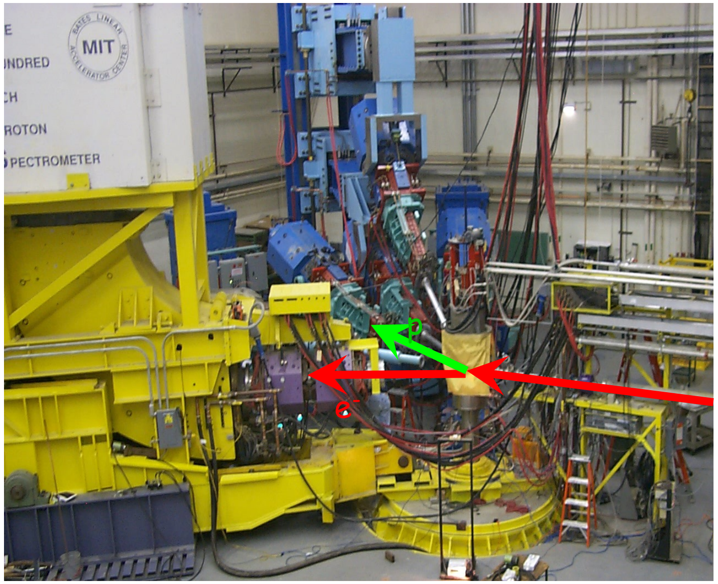

MAMI-A1 @ Q^2=0.33 GeV^2

Jlab-Hall A @ Q^2=0.9 & 1.8 GeV^2

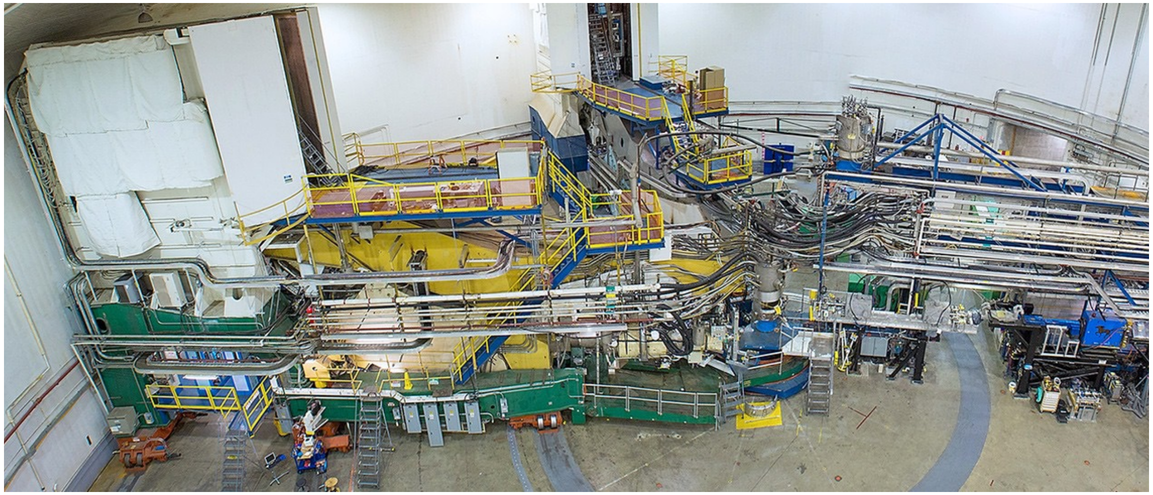

Early Experiments

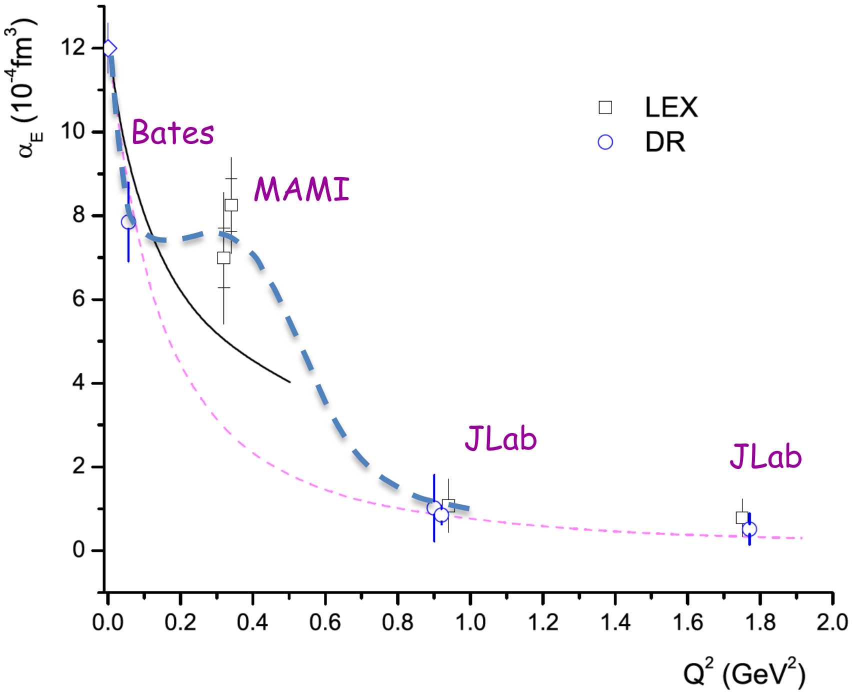

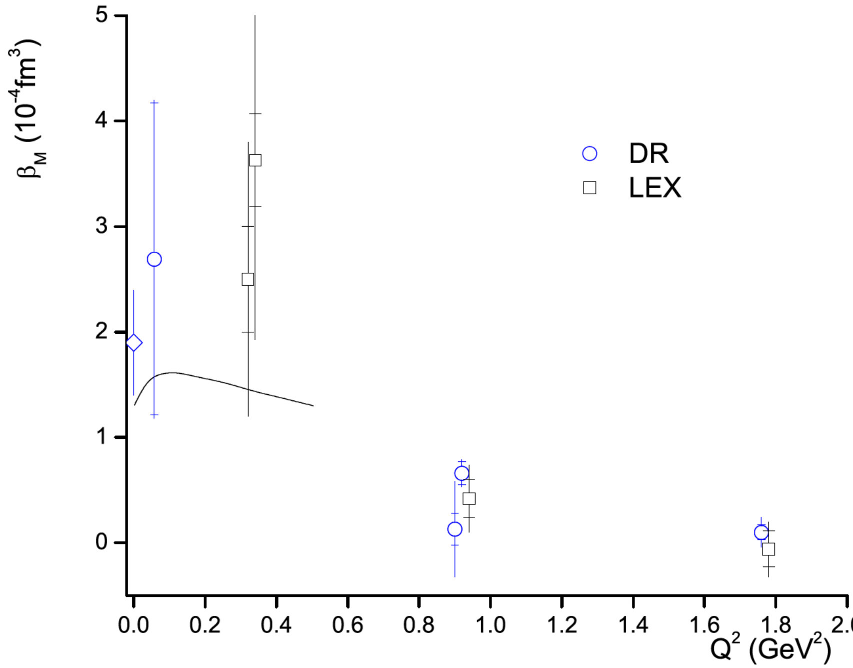

$\alpha_E \approx 10^{-3}\, V_N$ (stiffness / relativistic character)

Data: non-trivial Q^2 dependence of α_E (?)

Theory: monotonic fall-off

Q^2 = 0.33 (GeV/c)^2 measured twice at MAMI:

- Phys. Rev. Lett 85, 708 (2000)
- Eur. Phys. J. A37, 1-8 (2008)

β_M small ←→ cancellation of competing mechanisms

Large uncertainties

Higher precision measurements needed

→ Quantify the balance between diamagnetism and paramagnetism

Theory

HBChPT	T.R. Hemmert et al	Phys. Rev. D 62, 014013 (2000)
NRQCM	B. Pasquini et al	Phys. Rev. C 63, 025205 (2001)
Effective Lagrangian Model	A. Yu. Korchin and O. Scholten	Phys. Rev. C 58, 1098 (1998)
Linear Sigma Model	A. Metz and D. Drechsel	Z. Phys. A 356, 351 (1996)

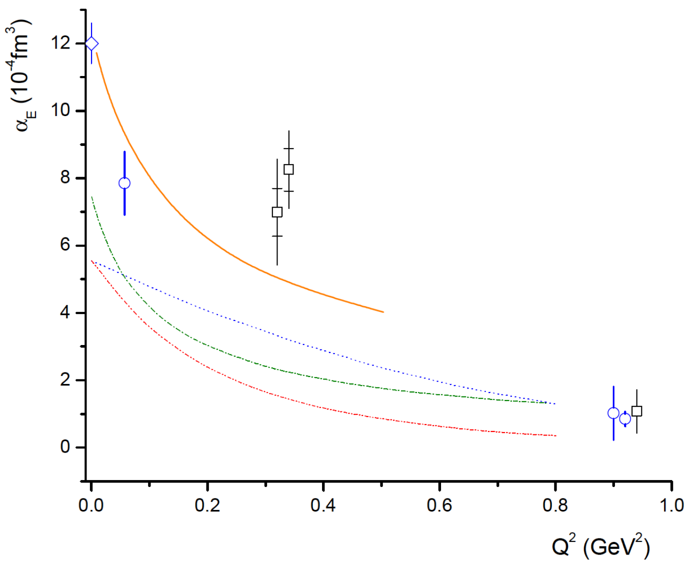

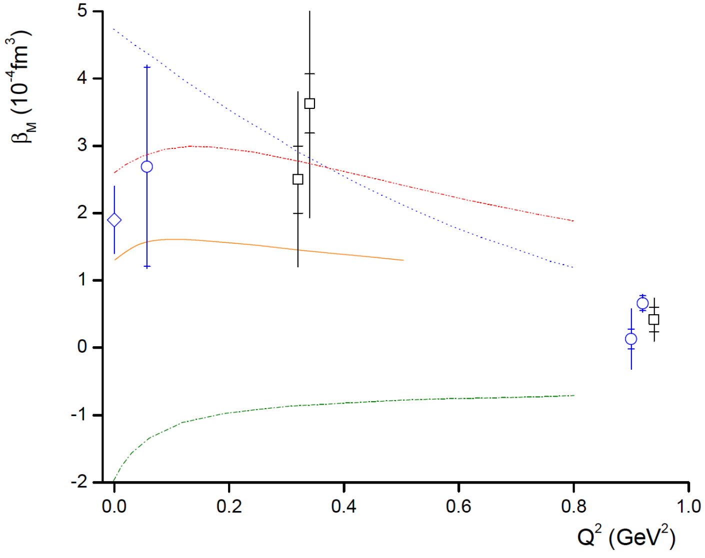

Smooth fall-off for α_E

A non-trivial structure for α_E is not supported by theory

Large spread in the predictions of the magnetic GP

Recent Measurements

Recent Measurements: MAMI

MAMI A1/1-09 (vcsq2) below threshold

MAMI A1/3-12 (vcsdelta) above threshold

Both experiments utilized the A1 setup at MAMI

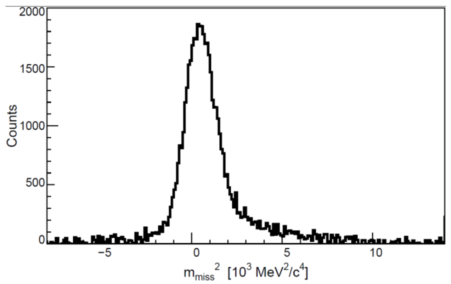

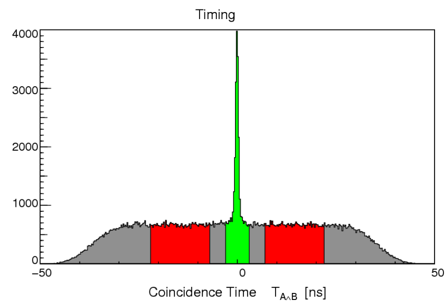

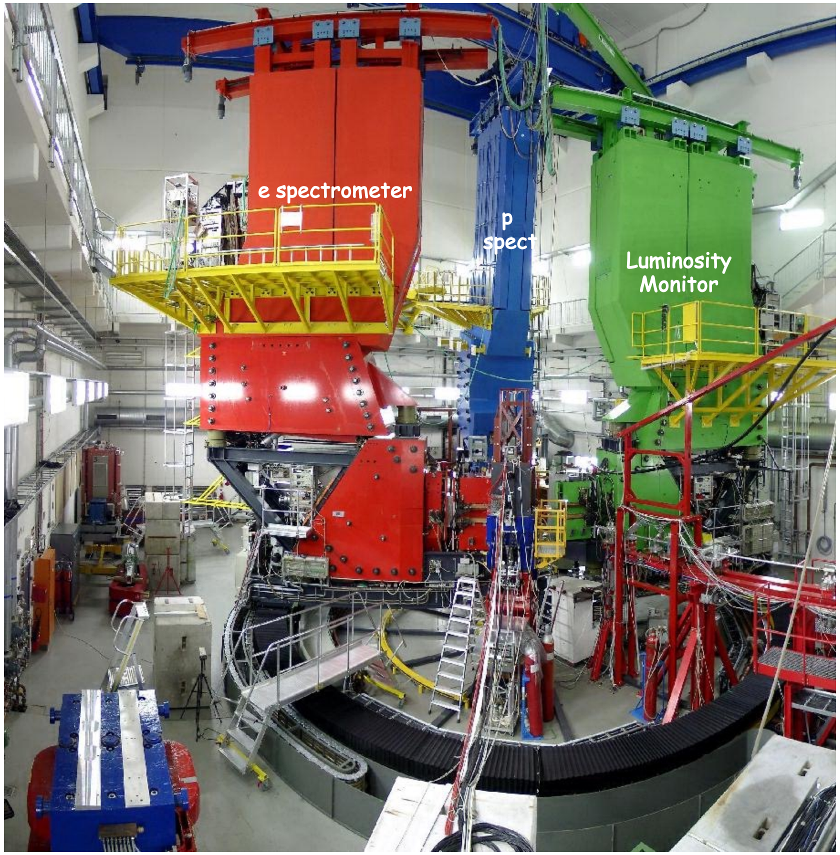

A1/1-09 @ MAMI

For LEX the higher order terms have to be kept small / under control

$$d^5\sigma \;=\; d^5\sigma^{BH+Born} \;+\; q'_{cm}\cdot\phi\cdot\Psi_0 \;+\; \mathcal{O}(q'^2_{cm})$$

Refined analysis procedure / phase space masking to keep these terms smaller than ~ 2%-3% level

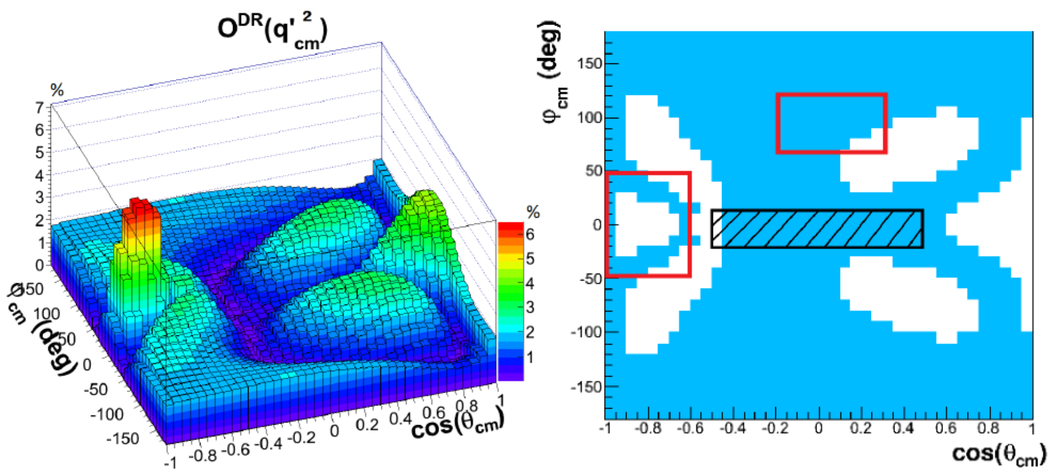

Figure 3.13: (Left) behavior of $\mathcal{O}^{DR}({q'_{cm}}^2)$ in the $(cos(\theta_{cm}),\varphi_{cm})$-plane at $q'_{cm} = 87.5\ MeV/c$ and (right) two-dimensional representation of the angular region where $\mathcal{O}^{DR}({q'_{cm}}^2) < 2\%$ (blue), the red squares correspond to the two areas of interest to perform the GP extraction.

Figure from PhD thesis of L. Correa, Mainz / Cl. Ferrand

MAMI Results

Phys. Rev. Lett 123, 192302

Phys. Rev. C 103, 025205

Eur. Phys. J. A55, 182

PhD students:

Jure Bericic (Ljubljana Univ.)

Loup Correa (Clermont-Fd Univ.)

Meriem BenAli (Clermont-Fd Univ.)

Adam Blomberg (Temple Univ.)

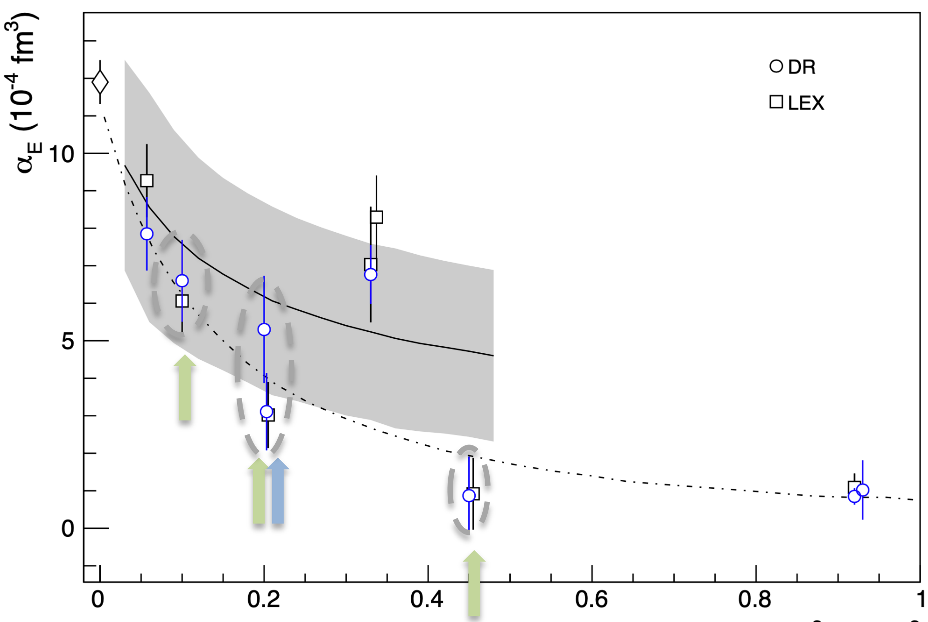

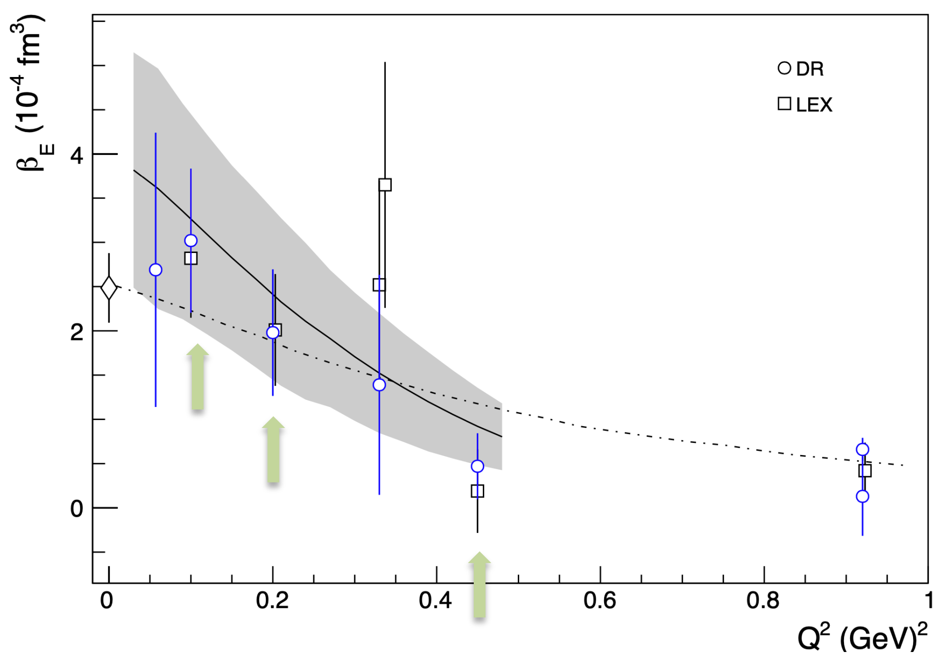

A1/1-09 @ MAMI

A1/3-12 @ MAMI

Revisiting the Q^2=0.33 GeV^2 data

Q^2 = 0.33 $(GeV/c)^2$ measured twice at MAMI - two different experiments

- Phys. Rev. Lett 85, 708 (2000)
- Eur. Phys. J. A37, 1-8 (2008)

Analysis revisited (unpublished):

$\alpha_E(Q^2)$

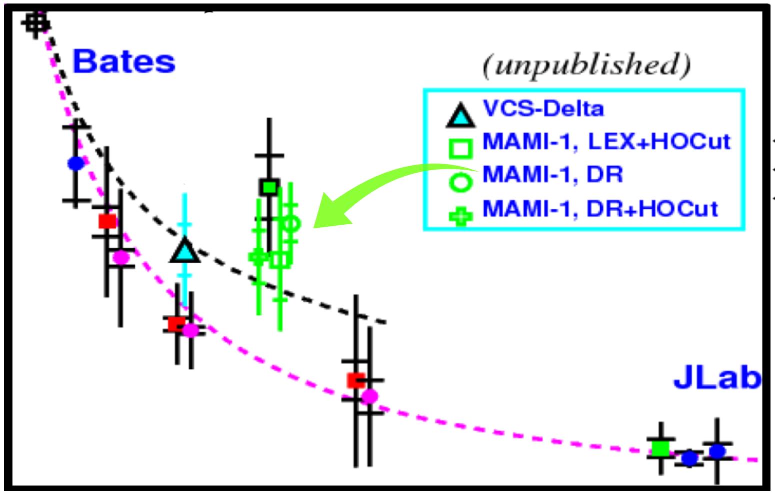

Re-fits at Q^2=0.33 GeV^2 (H.F.)

LEX and DR

Updated HO-cut

The α_E puzzle still holds

$\beta_M(Q^2)$

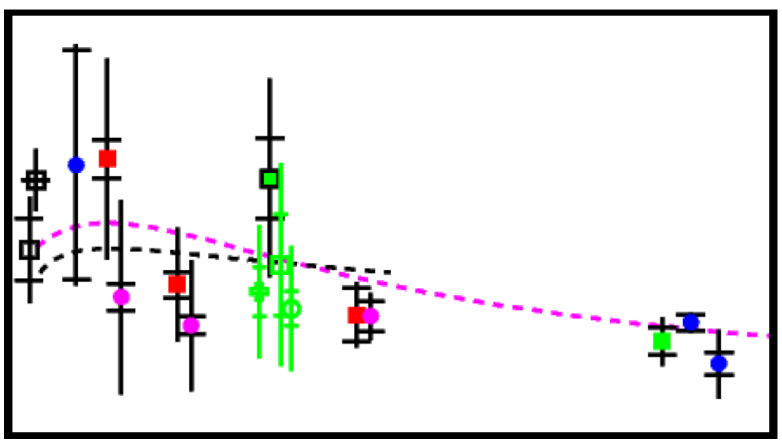

(material from H. Fonvieille)

Jlab : Experiment E12-15-001 (VCS-I) in Hall C

High precision measurements targeting
explicitly the kinematics of interest for α_E

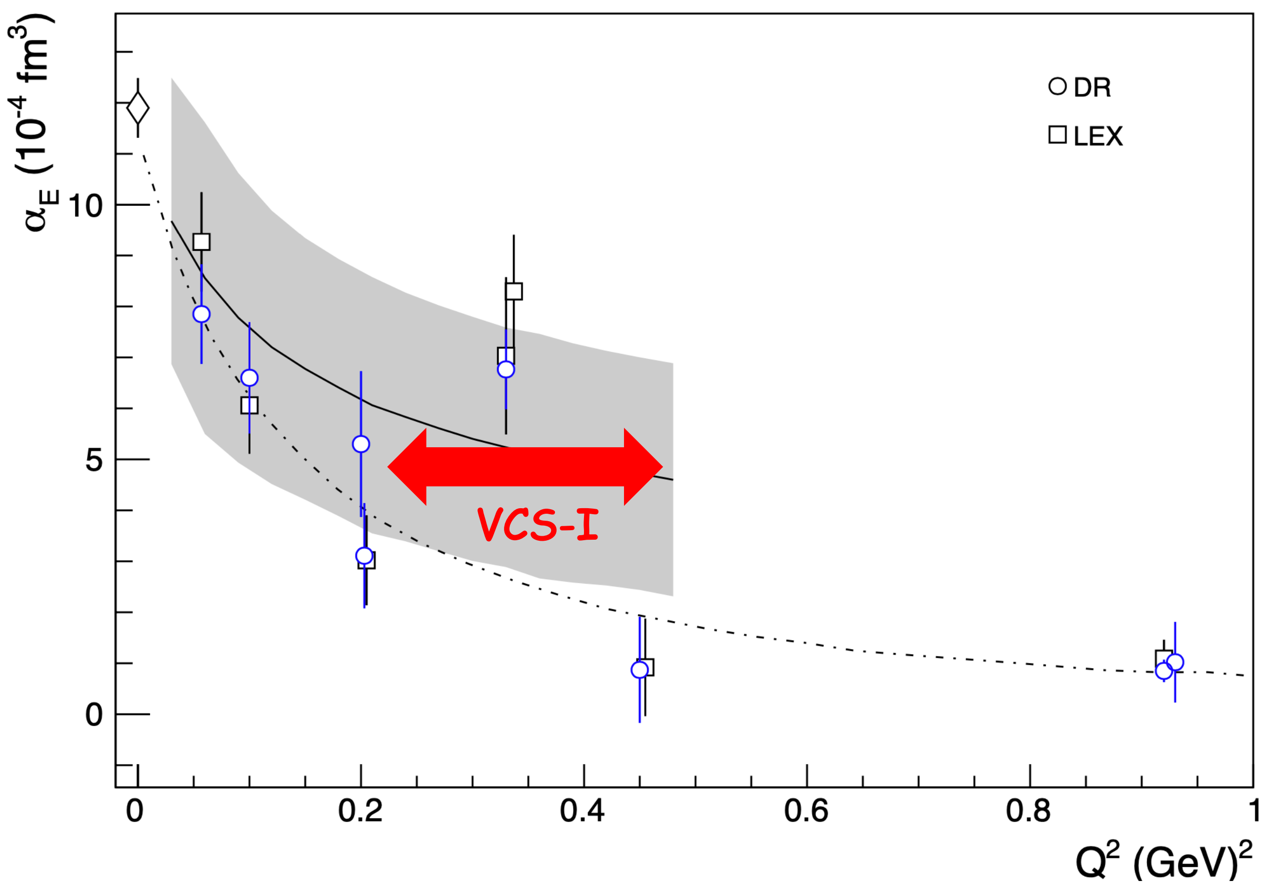

Hall C HMS and SHMS

SHMS:
- 11-GeV Spectrometer
- Partner of existing 6-GeV **HMS**

MAGNETIC OPTICS:
- Point-to Point QQQD for easy calibration and wide acceptance.
- Horizontal bend magnet allows acceptance at forward angles (5.5°)

Detector Package:
- Drift Chambers
- Hodoscopes
- Cerenkovs
- Calorimeter
- All derived from existing HMS/SOS detector designs

- Super High Momentum Spectrometer
  - HB, 3 Quads, Dipole
  - P ➛ 2 - 11 GeV
  - Resolution: $\delta < 0.1\%$
  - Acceptance: δ ➛30%, 4 msr
  - $5.5° < \theta < 40°$
  - Good e/π/K/p PID
- High Momentum Spectrometer
  - 3 Quads, Dipole
  - P ➛ 7.5 GeV
  - Resolution: $\delta < 0.1\%$
  - Acceptance: δ ➛18%, 6.5 msr
  - $10.5° < \theta < 90°$
  - Good e/π/K/p PID

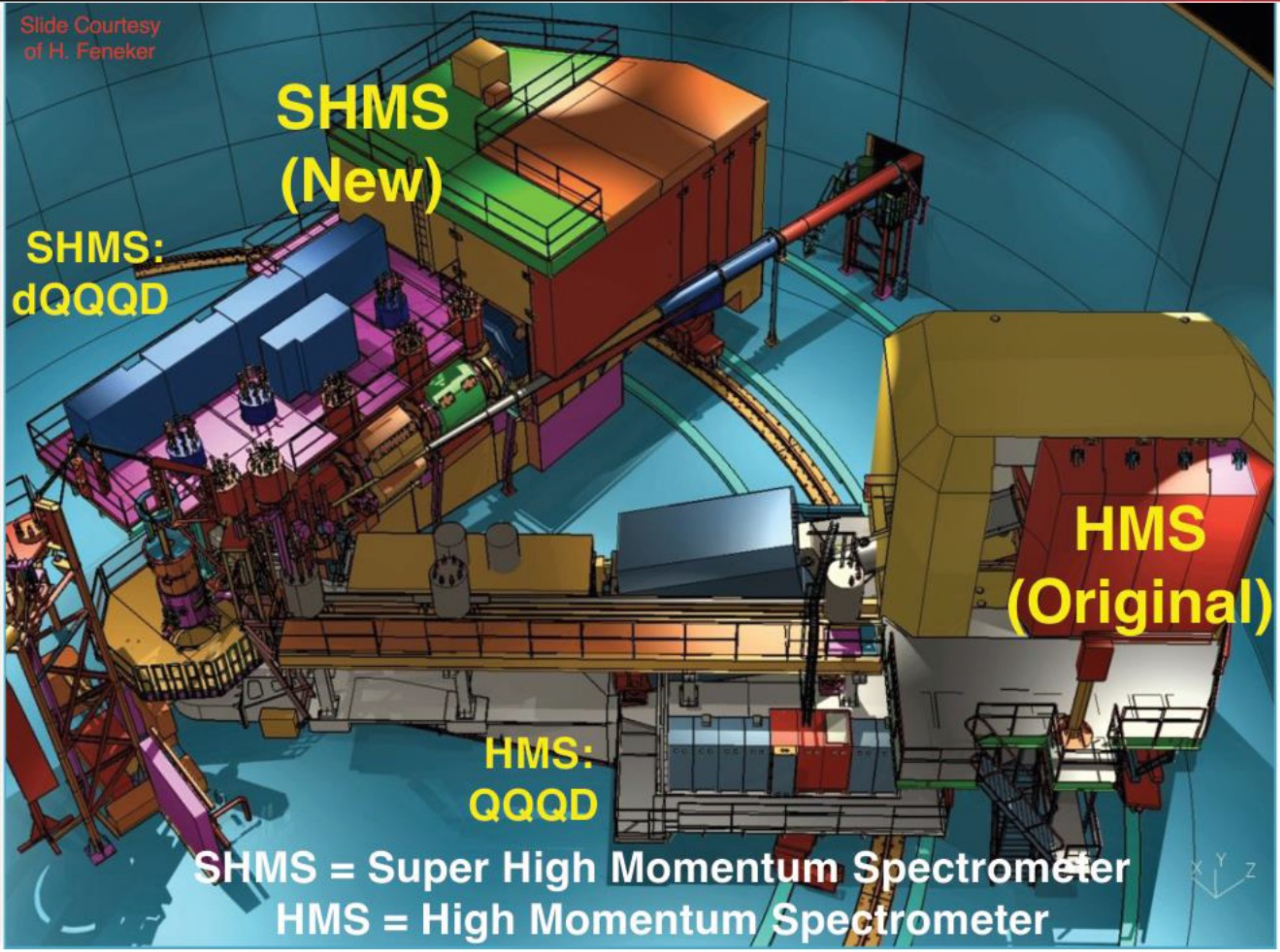

The experiment

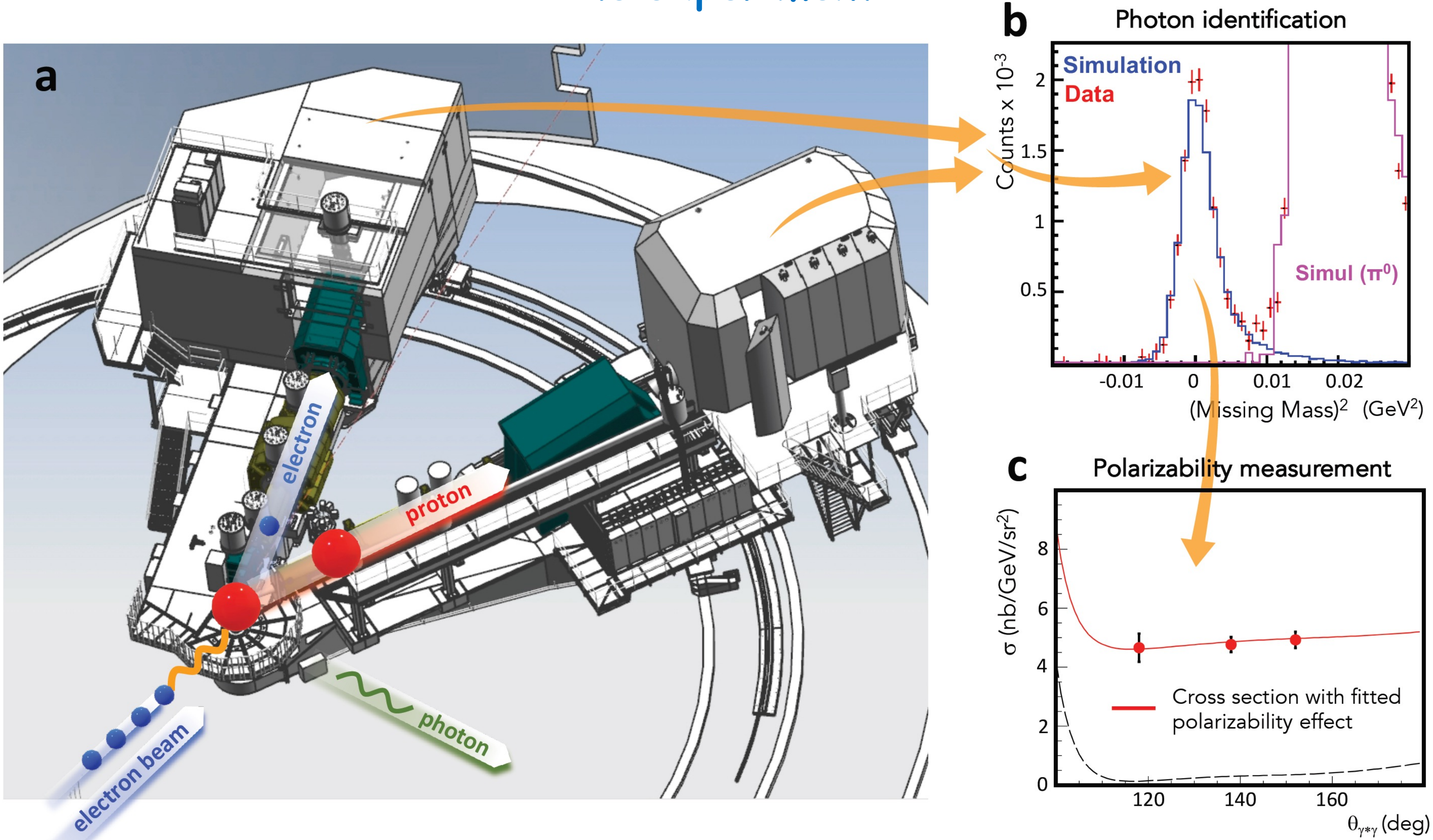

Hall C:

- SHMS, HMS
- 4.56 GeV
- 20 μA
- Liquid hydrogen 10 cm

cross sections & azimuthal asymmetries

$$A_{(\phi_{\gamma^*\gamma}=0,\pi)} = \frac{\sigma_{\phi_{\gamma^*\gamma}=0} - \sigma_{\phi_{\gamma^*\gamma}=180}}{\sigma_{\phi_{\gamma^*\gamma}=0} + \sigma_{\phi_{\gamma^*\gamma}=180}}$$

sensitivity to GPs

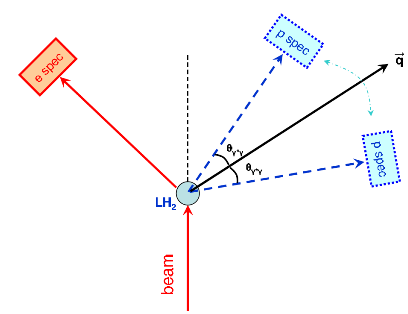

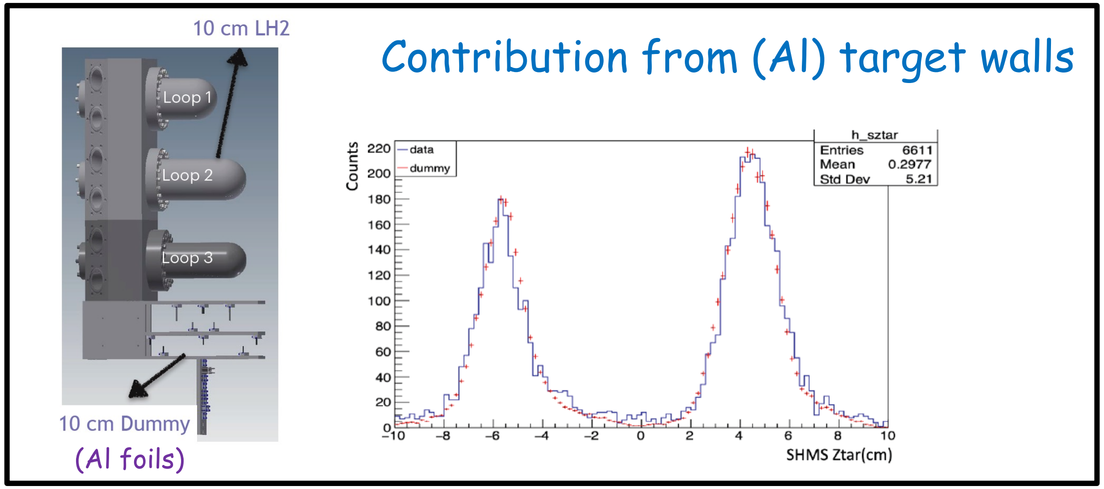

Contribution from (Al) target walls
10 cm LH2
Loop 1
Loop 2
Loop 3
10 cm Dummy
(Al foils)
data
dummy
h_sztar
Entries 6611
Mean 0.2977
Std Dev 5.21
Counts
SHMS Ztar(cm)

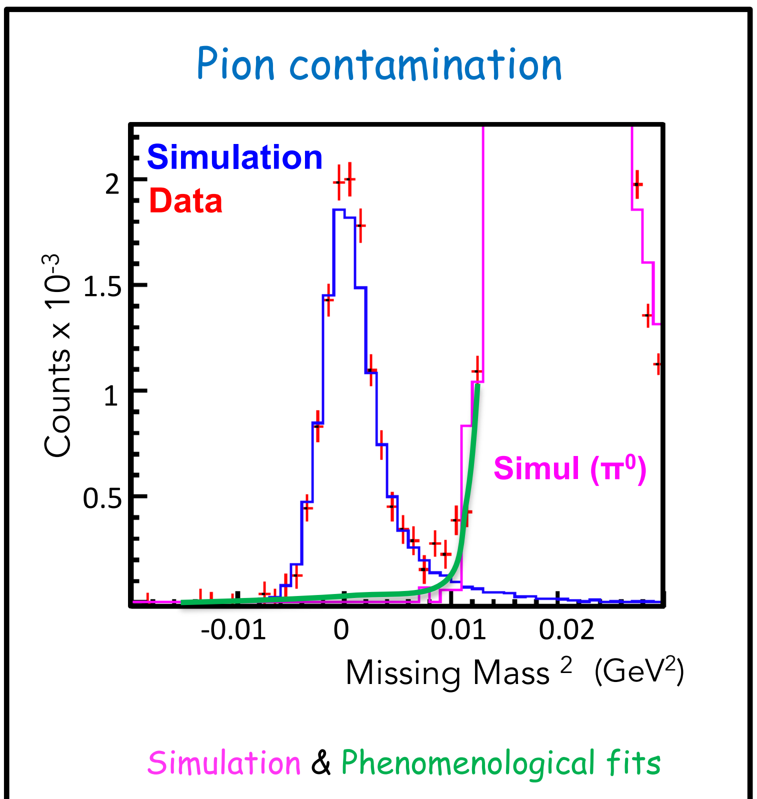

Pion contamination
Simulation
Data
Simul (π⁰)
Counts x 10⁻³
Missing Mass ² (GeV²)
Simulation & Phenomenological fits

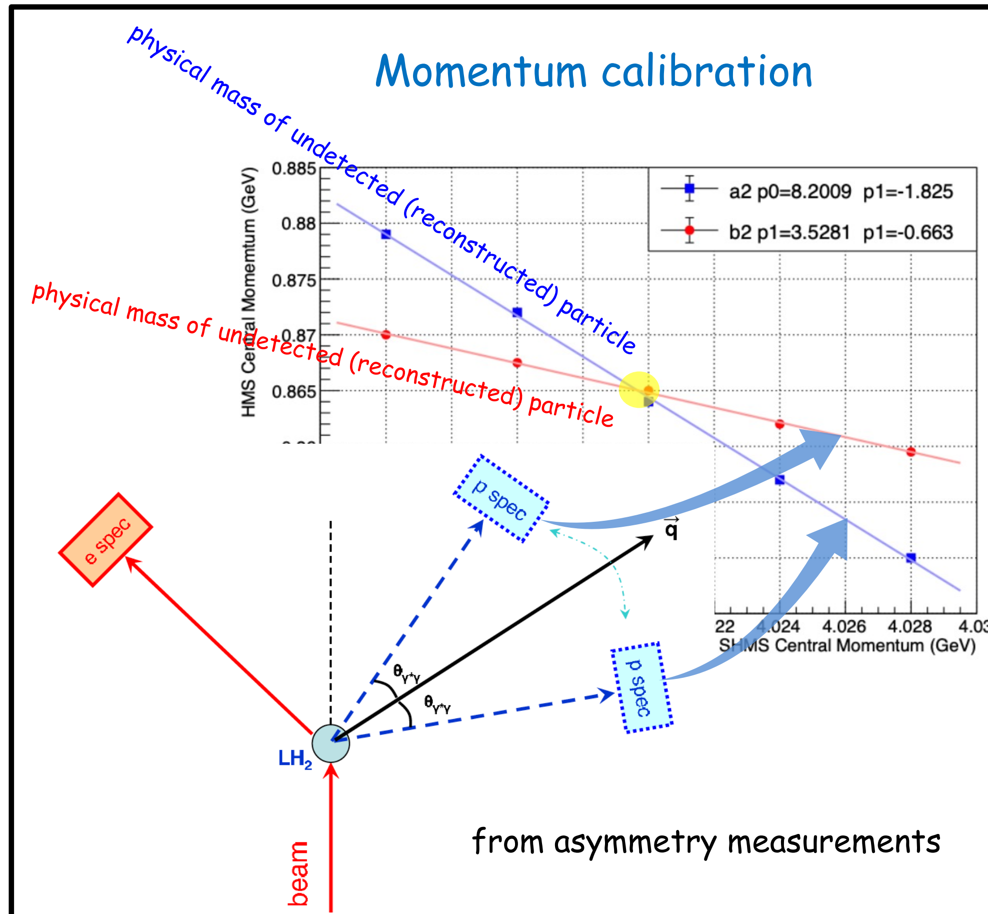

Momentum calibration
physical mass of undetected (reconstructed) particle
physical mass of undetected (reconstructed) particle
a2 p0=8.2009 p1=-1.825
b2 p1=3.5281 p1=-0.663
HMS Central Momentum (GeV)
SHMS Central Momentum (GeV)
p spec
p spec
e spec
LH2
beam
from asymmetry measurements

Elastic data

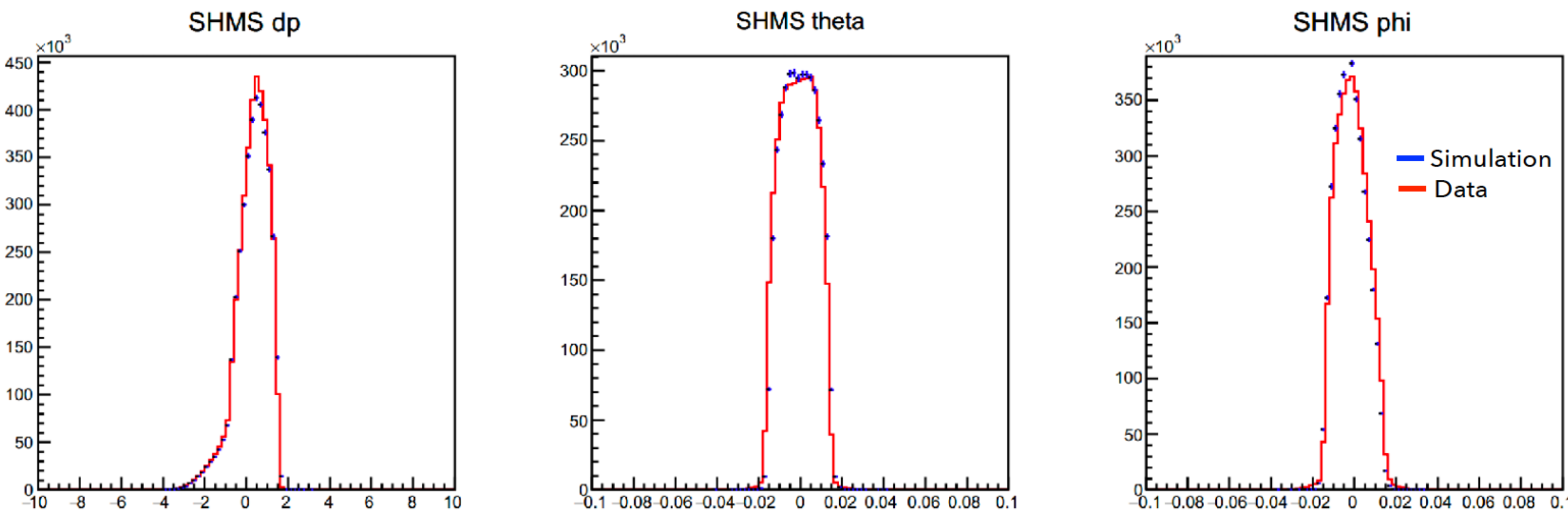

Kinematic	θ_e°	$P_e(GeV/c)$	θ_p°	$P_p(GeV/c)$
Elastic I	10.76	4.193	61.16	0.893
Elastic II	10.41	4.214	61.95	0.863
Elastic III	9.64	4.259	63.76	0.795

$p(e,e'p)\pi^0$

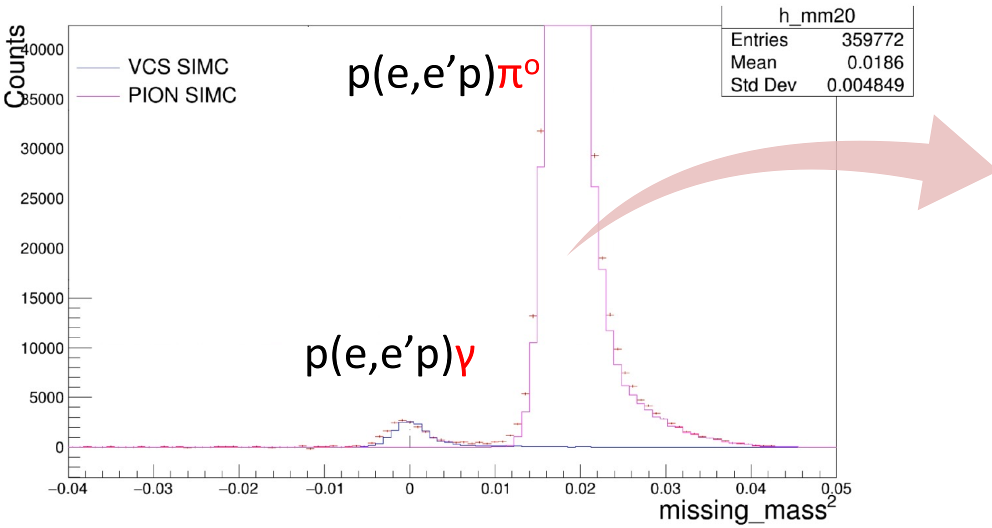

VCS SIMC
PION SIMC
p(e,e'p)π°
p(e,e'p)γ
h_mm20
Entries 359772
Mean 0.0186
Std Dev 0.004849
Counts
missing_mass²

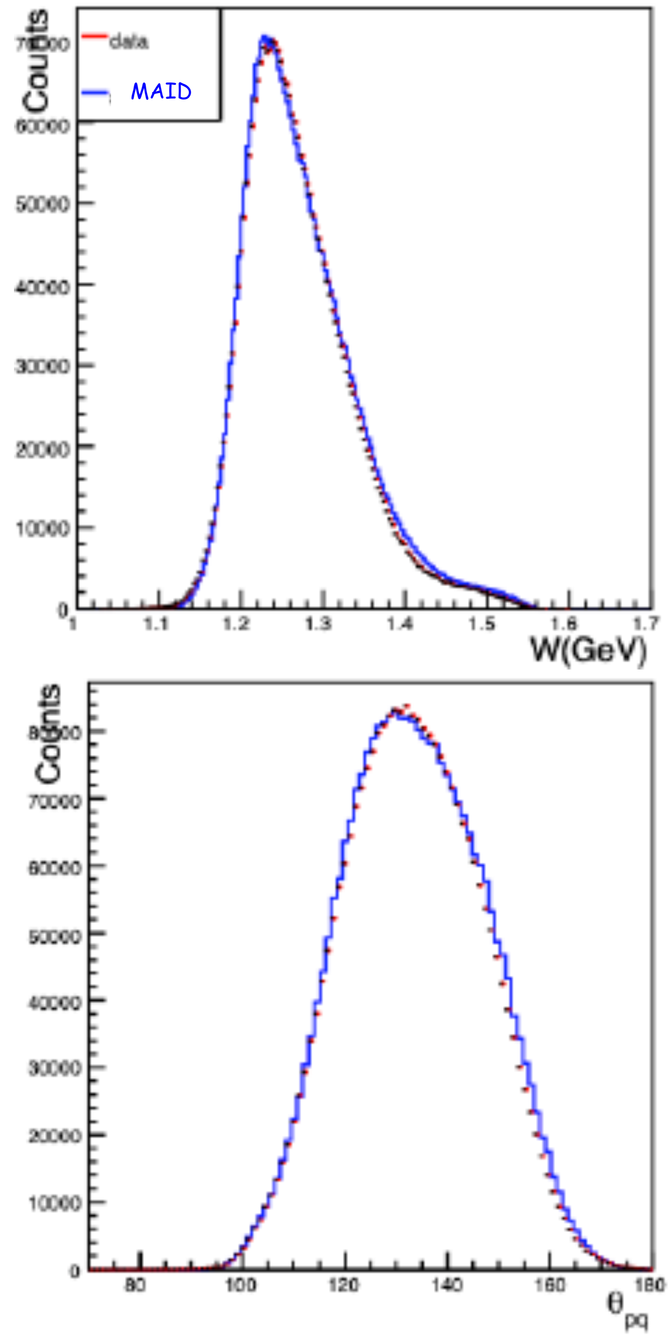

data
MAID
Counts
W(GeV)
Counts
θ_pq

N→Δ TFFs

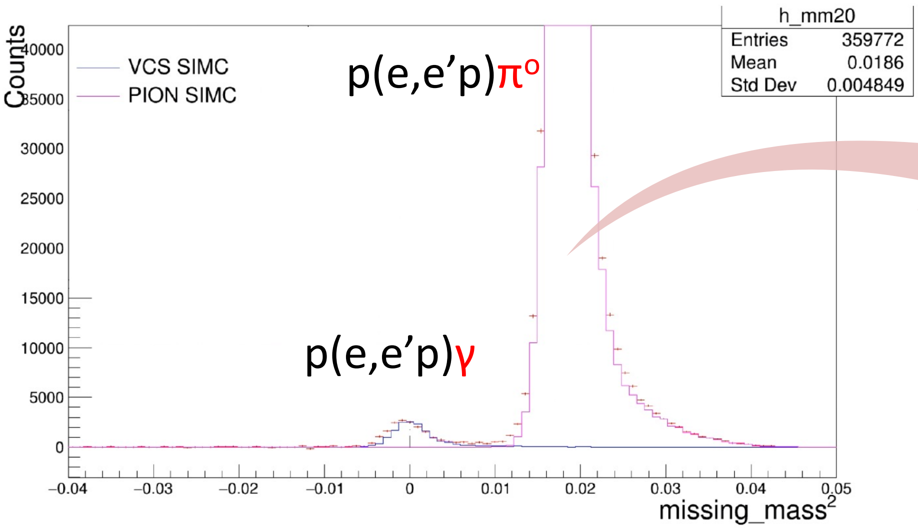

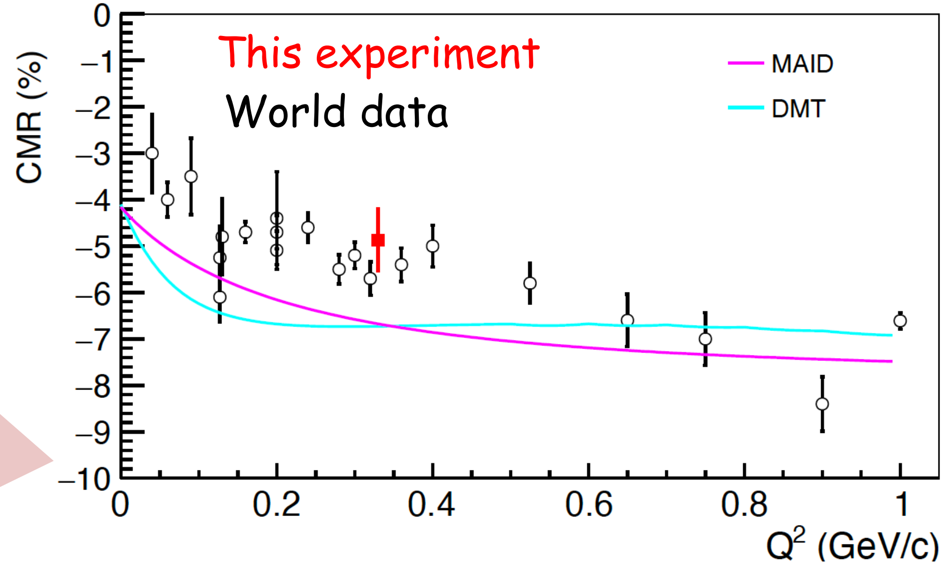

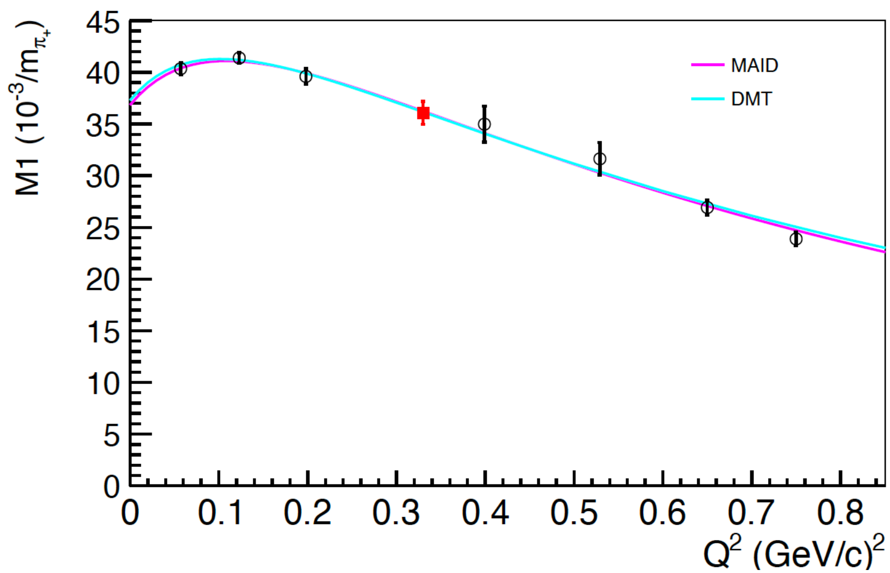

Simultaneous measurement
of the N→Δ TFFs

TFFs well known
→ Real time normalization control

Good understanding of
spectrometer acceptance

New results: VCS cross sections

Q^2=0.27 GeV^2

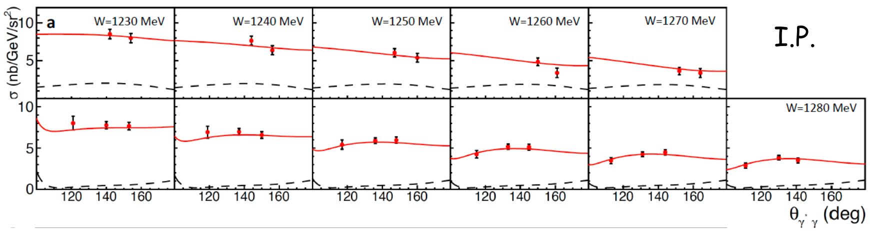

I.P.

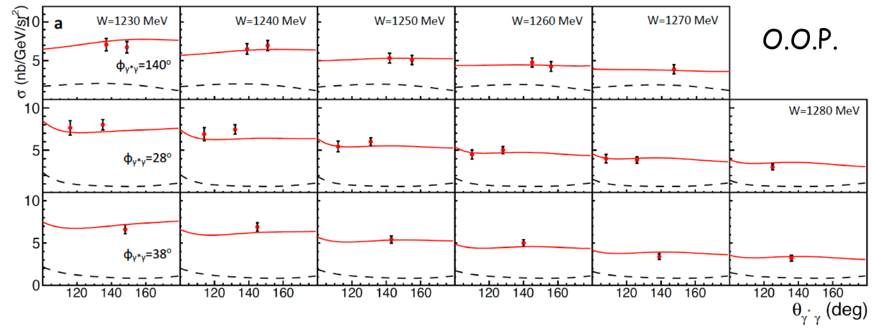

O.O.P.

Q^2=0.33 GeV^2

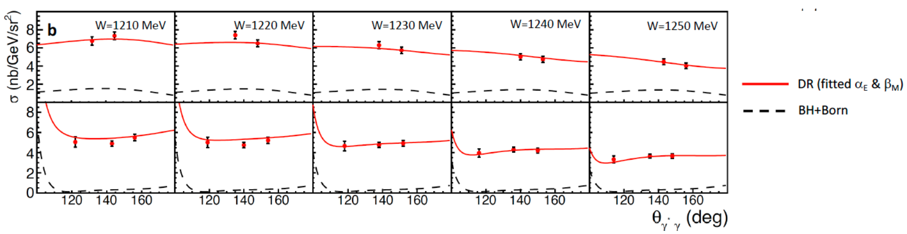

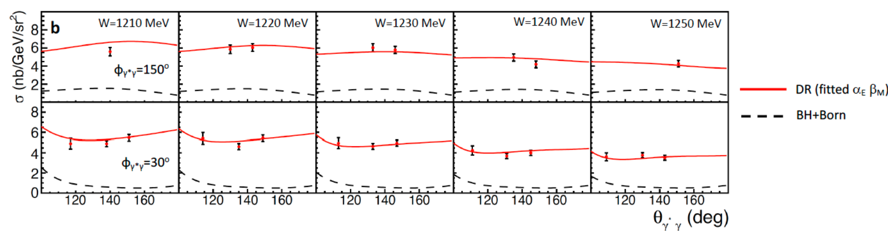

Q^2=0.40 GeV^2

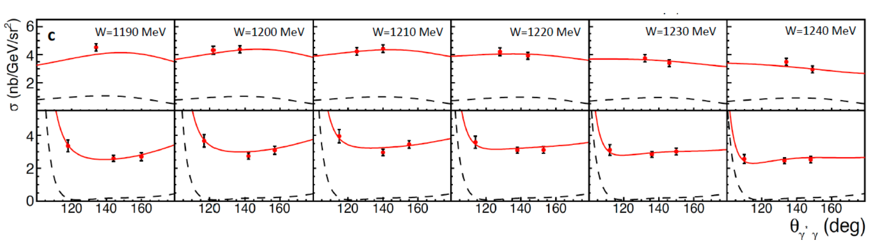

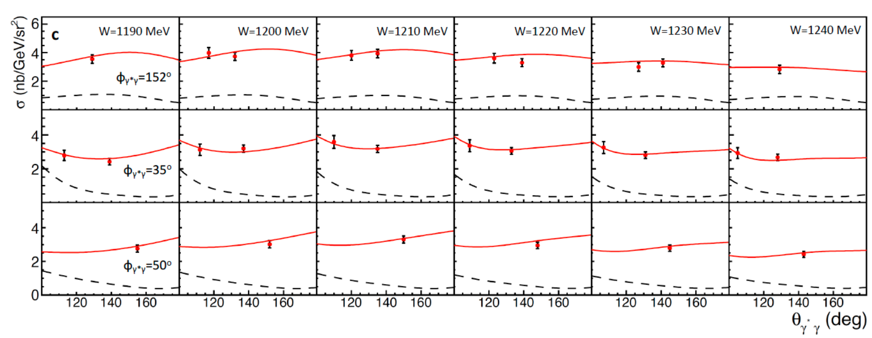

New results: GPs

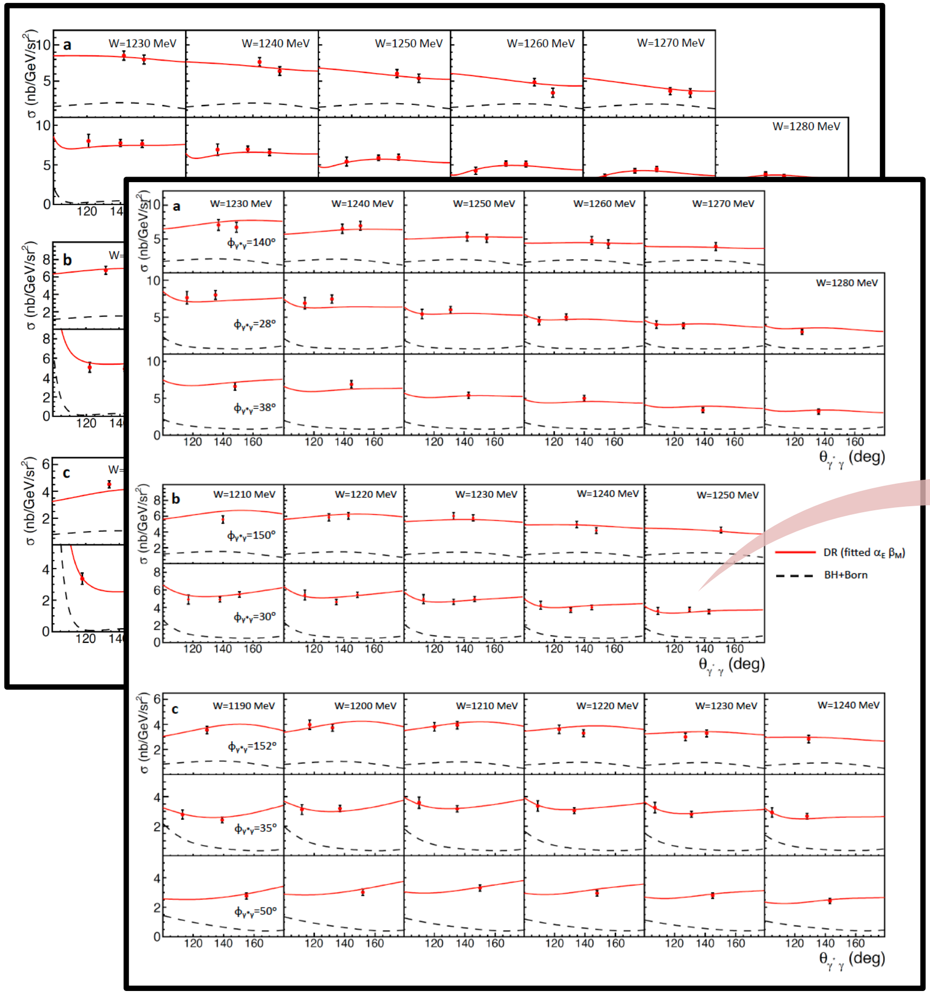

DR fit

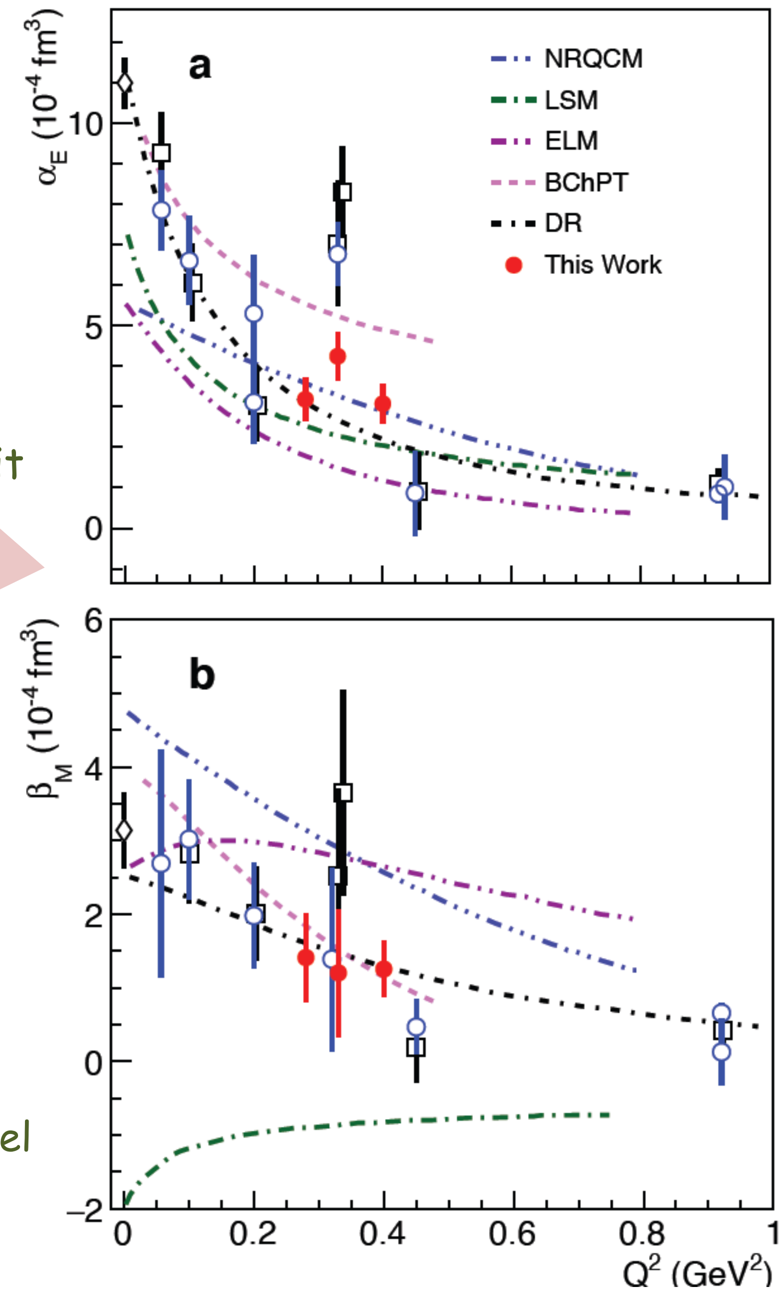

Experimental cross sections are compared to the DR model predictions for all possible values for the GPs

→ $\alpha_E(Q^2)$ and $\beta_M(Q^2)$ are fitted by a χ^2 minimization

New results: GPs

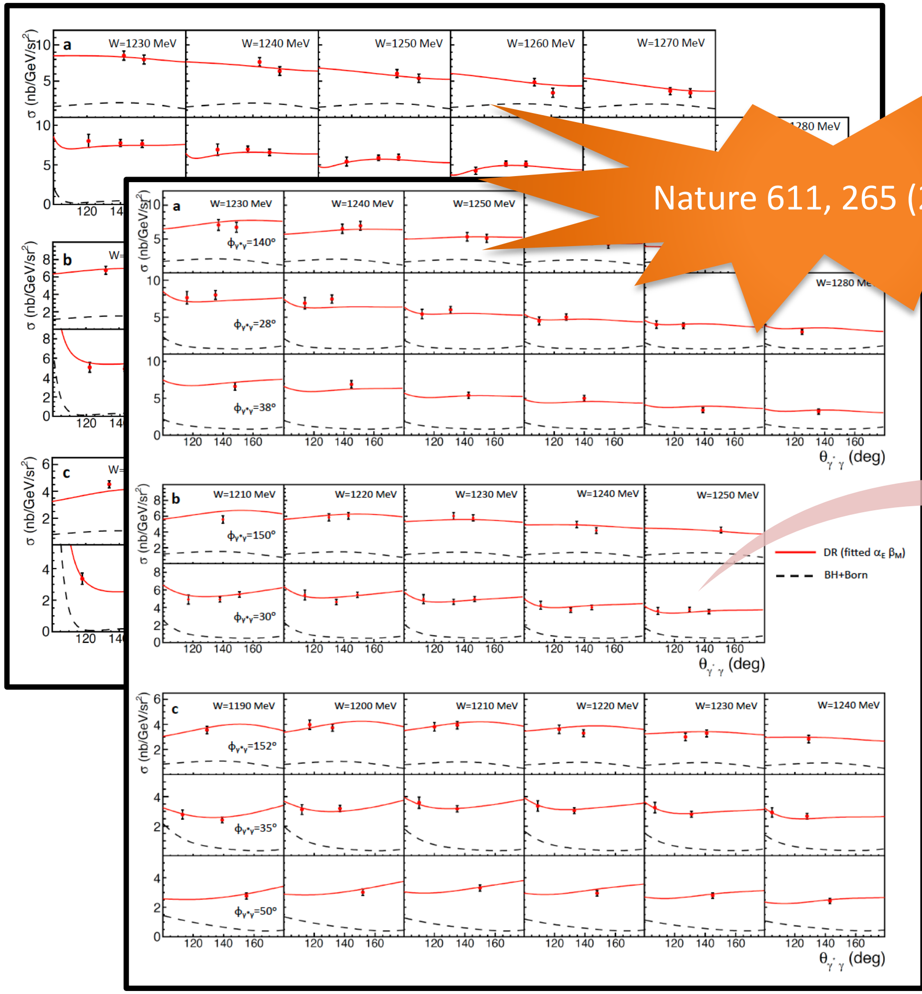

Nature 611, 265 (2022)

DR fit

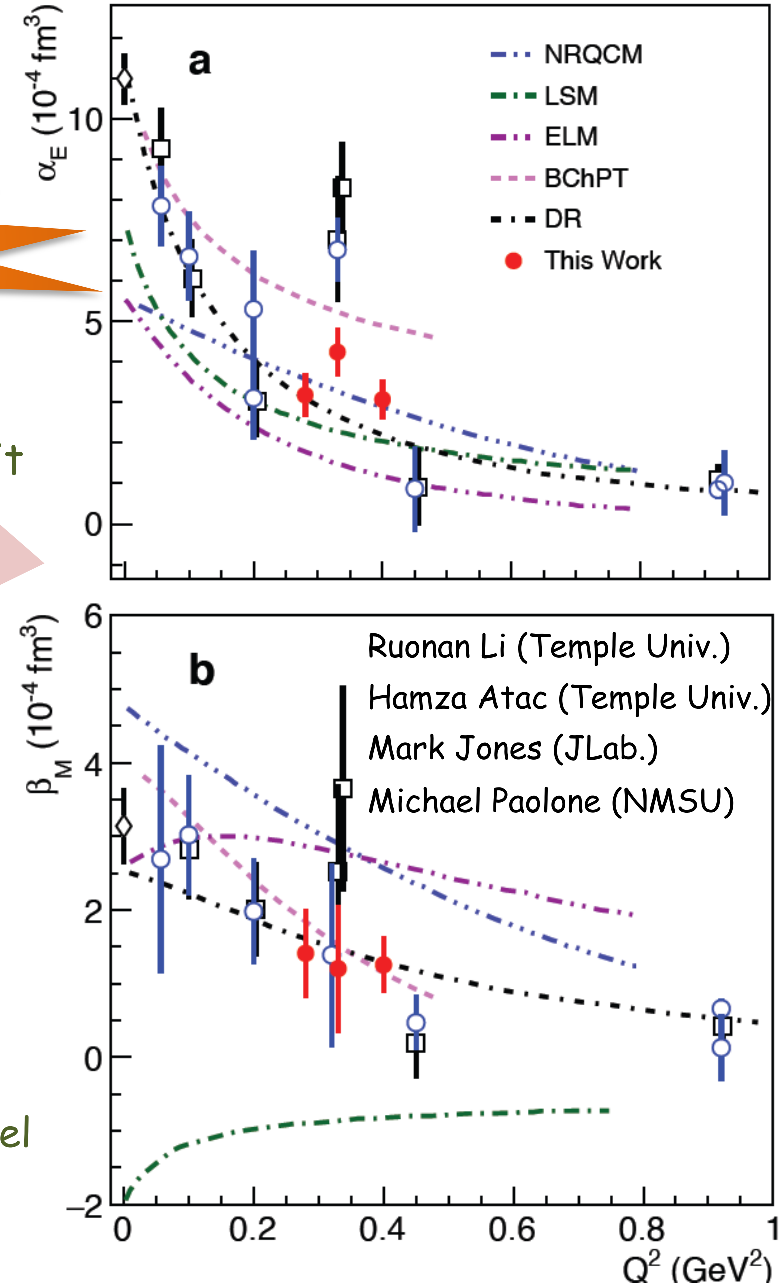

Experimental cross sections are compared to the DR model predictions for all possible values for the GPs

→ $\alpha_E(Q^2)$ and $\beta_M(Q^2)$ are fitted by a χ^2 minimization

MAMI-I re-analysis (unpublished)

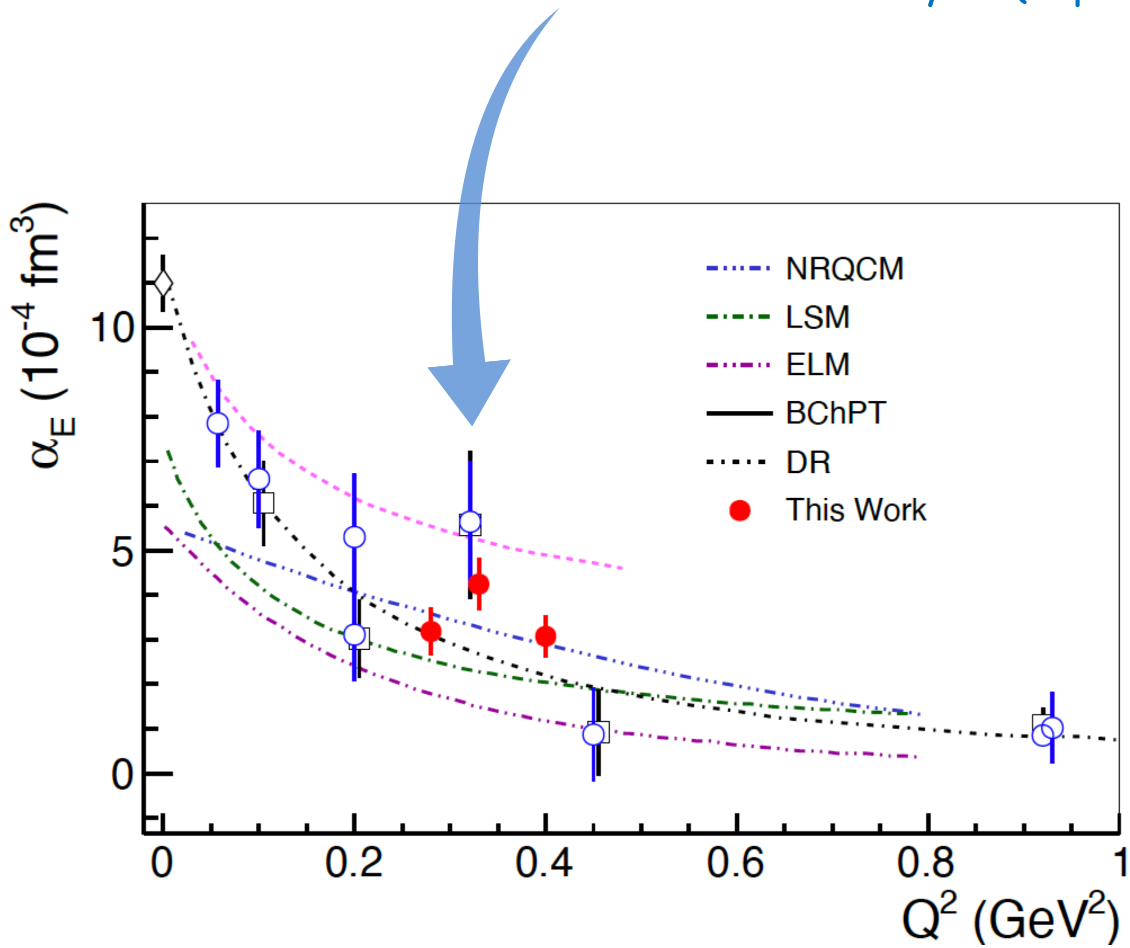

Is there a non-trivial structure?

Electric GP

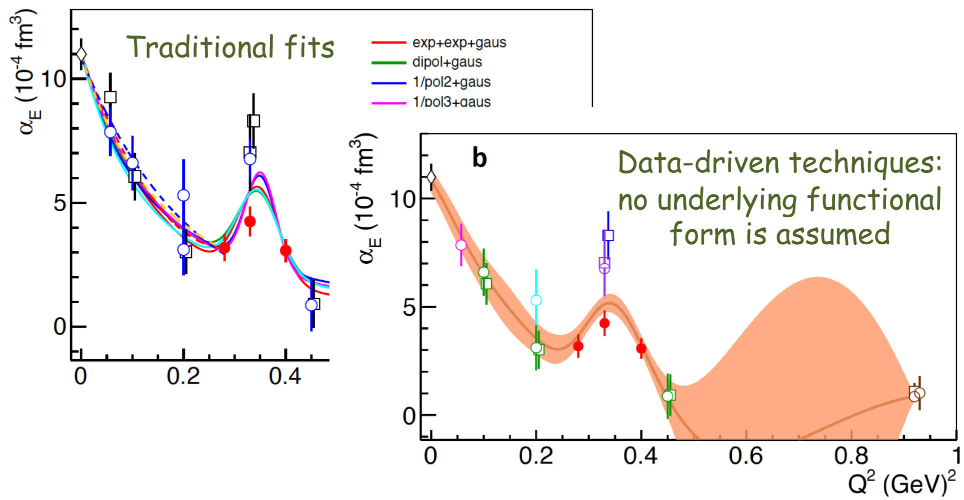

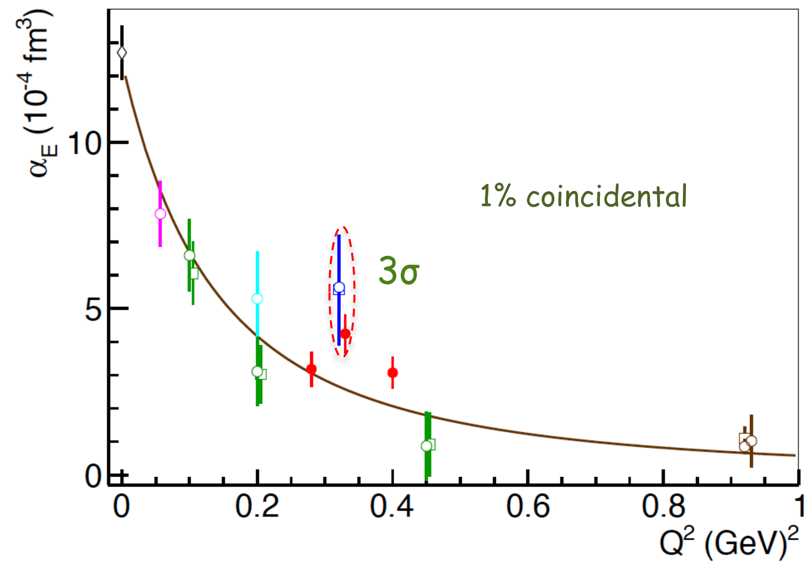

Is the observed α_E structure coincidental or not?

If true: Measure the shape precisely → input to theory

If not: We are able to show it with more measurements

Strong tension between world data (?)

Things we do not yet understand well?

Underestimated uncertainties? …

Magnetic GP

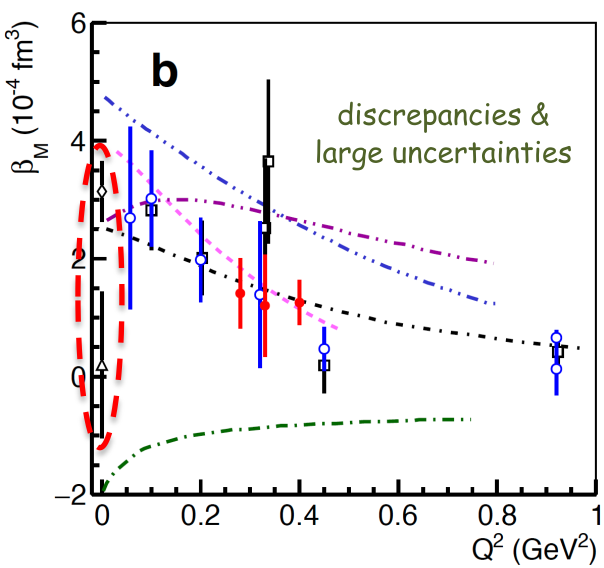

Magnetic GP: Large uncertainties & discrepancies

Instrumental to disentangle diamagnetism and paramagnetism in the proton

Unique opportunity to measure α_E and β_M with superb precision and with consistent systematics across Q^2

Theory: BχPT

Eur. Phys. J. C (2017) 77:119
DOI 10.1140/epjc/s10052-017-4652-9

THE EUROPEAN PHYSICAL JOURNAL C

Regular Article - Theoretical Physics

Generalized polarizabilities of the nucleon in baryon chiral perturbation theory

Vadim Lensky[1,2,3,a], Vladimir Pascalutsa[1], Marc Vanderhaeghen[1]
[1] Institut für Kernphysik, Cluster of Excellence PRISMA, Johannes Gutenberg Universität Mainz, 55128 Mainz, Germany
[2] Institute for Theoretical and Experimental Physics, Moscow 117218, Russia
[3] National Research Nuclear University MEPhI (Moscow Engineering Physics Institute), Moscow 115409, Russia

BχPT calculation to NLO in the δ-counting scheme

DR calculation
D. Drechsel, B. Pasquini, M. Vanderhaeghen, Phys. Rep. 378,99 (2003)

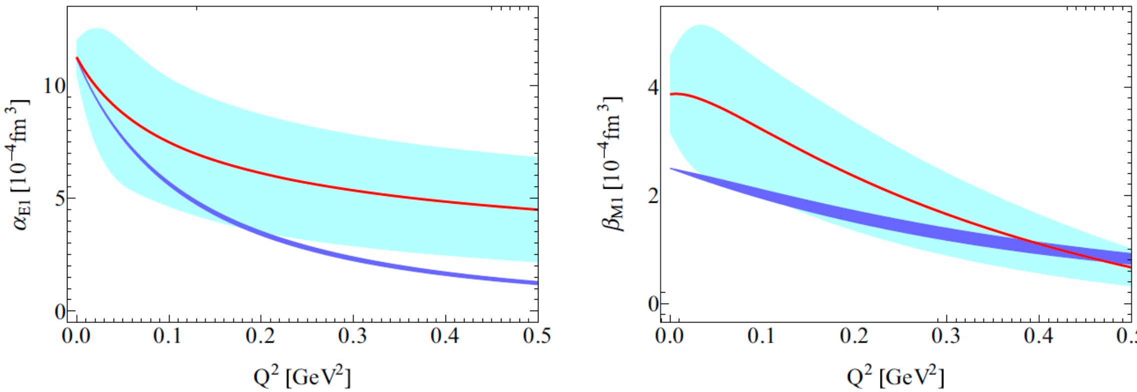

Theory: Lattice QCD

Lattice QCD results for the static polarizabilities

Next step: Lattice QCD calculations for the GPs

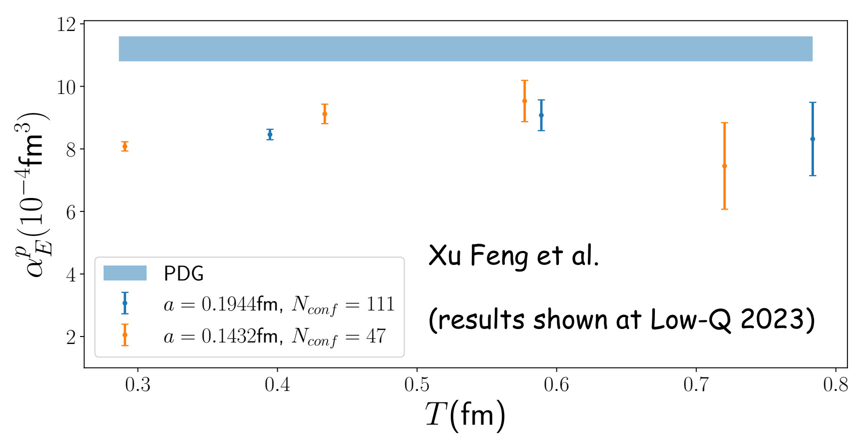

Spatial dependence of induced polarizations

Nucleon form factor data ➔ light-front quark charge densities

Formalism extended to the deformation of these quark densities when applying an external e.m. field:

GPs ➔ spatial deformation of charge & magnetization densities under an applied e.m. field

Induced polarization in a proton when submitted to an e.m. field

Phys. Rev. Lett. 104, 112001 (2010)

M. Gorchtein, C. Lorce, B. Pasquini, M. Vanderhaeghen

GP I

GP II

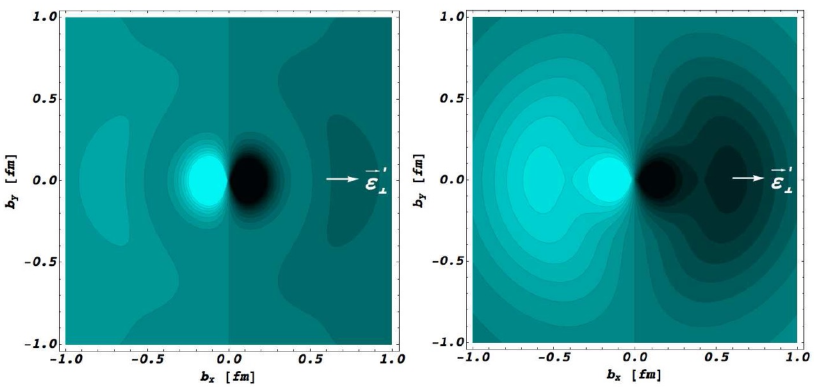

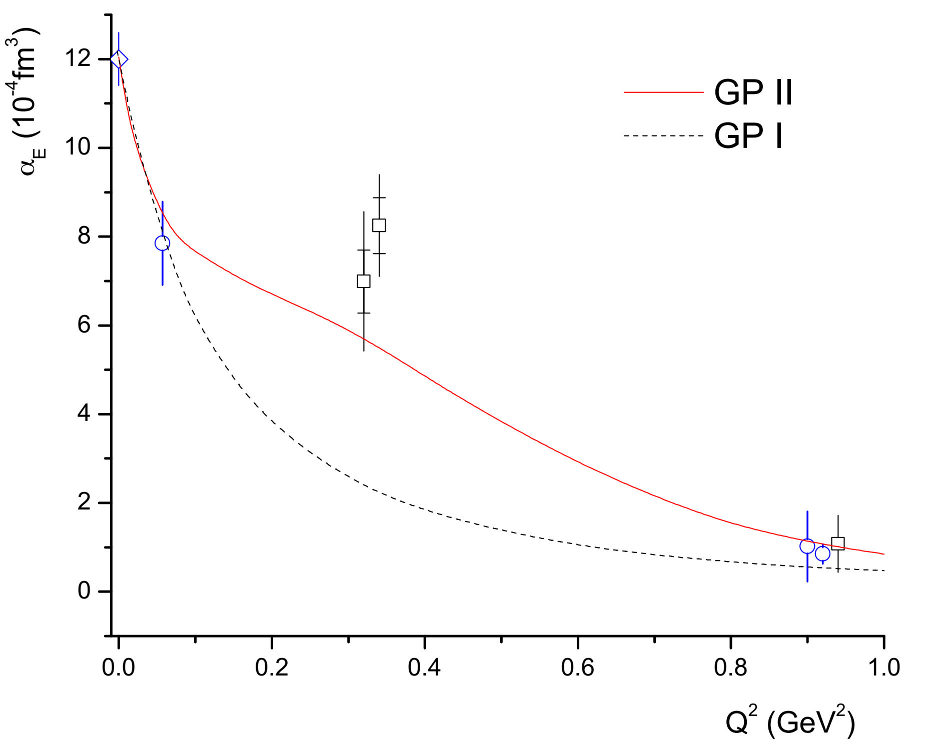

Light (**dark**) regions ➔ **largest** (**smaller**) values

(photon polarization along x-axis, as indicated)

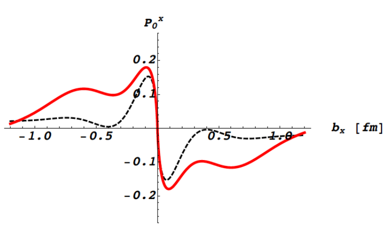

Induced polarization along b_y=0

Spatial dependence of induced polarizations

Nucleon form factor data ➔ light-front quark charge densities

Formalism extended to the deformation of these quark densities when applying an external e.m. field:

GPs ➔ spatial deformation of charge & magnetization densities under an applied e.m. field

Induced polarization in a proton when submitted to an e.m. field

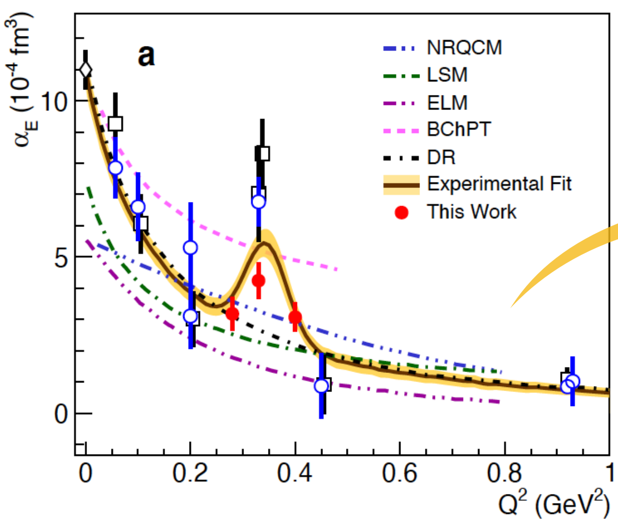

Experimental Fit

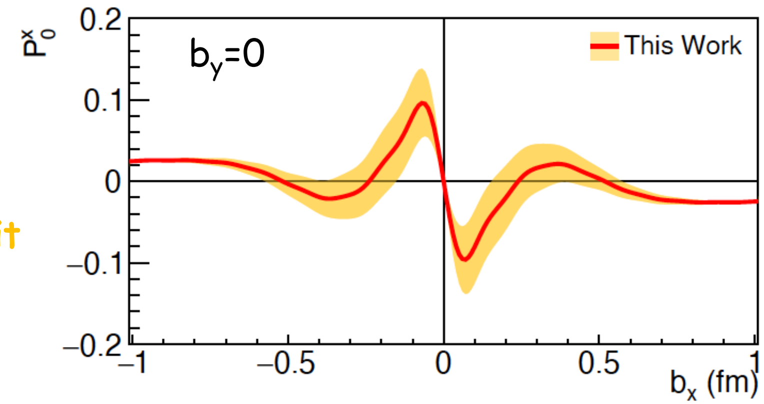

x-y defines the transverse plane with the z-axis being the direction of the fast-moving proton

Polarizability radii

$$\langle r^2_{\alpha_E} \rangle = \frac{-6}{\alpha_E(0)} \cdot \frac{d}{dQ^2} \alpha_E(Q^2) \Big|_{Q^2=0}$$

$$\langle r^2_{\beta_M} \rangle = \frac{-6}{\beta_M(0)} \cdot \frac{d}{dQ^2} \beta_M(Q^2) \Big|_{Q^2=0}$$

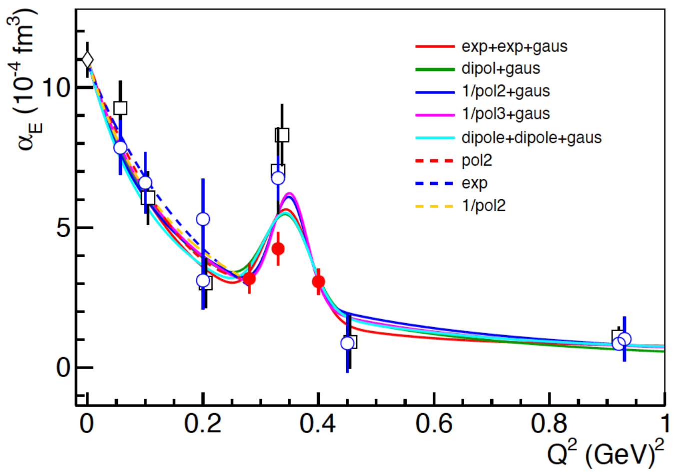

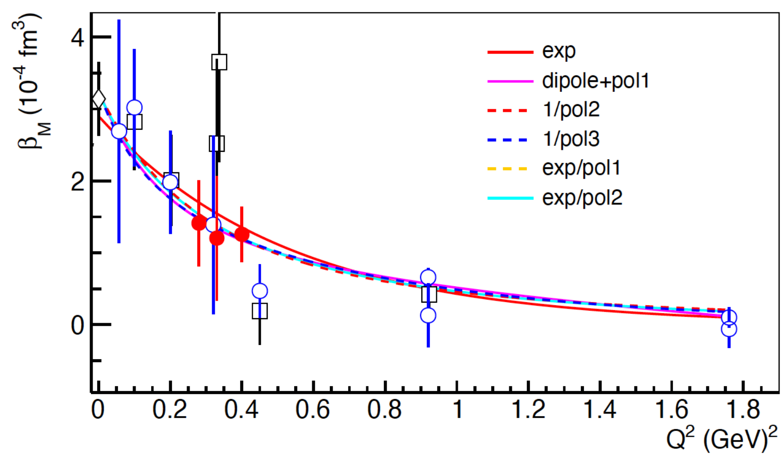

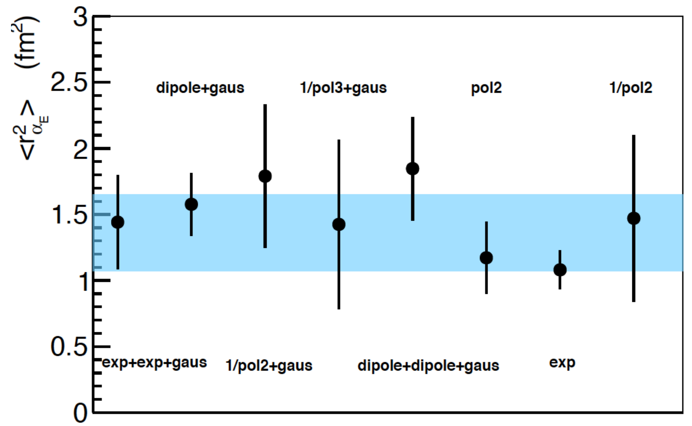

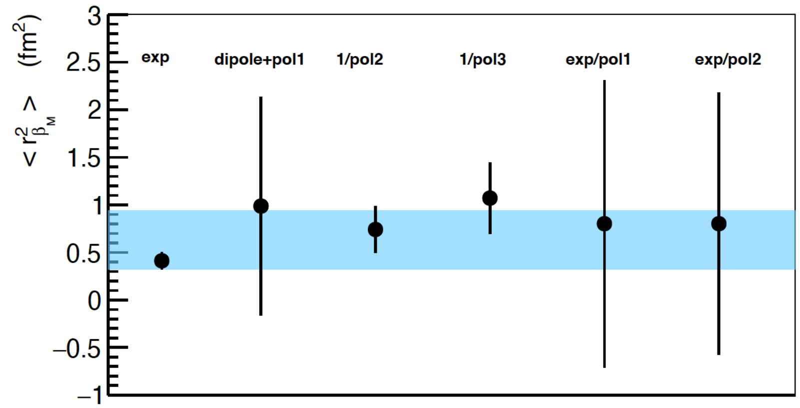

$$\langle r^2_{\alpha_E} \rangle = 1.36 \pm 0.29 \text{ fm}^2$$

$$\langle r^2_{\beta_M} \rangle = 0.63 \pm 0.31 \text{ fm}^2$$

Polarizability radii

$$\langle r^2_{\alpha_E} \rangle = \frac{-6}{\alpha_E(0)} \cdot \frac{d}{dQ^2}\alpha_E(Q^2)\Big|_{Q^2=0}$$

$$\langle r^2_{\beta_M} \rangle = \frac{-6}{\beta_M(0)} \cdot \frac{d}{dQ^2}\beta_M(Q^2)\Big|_{Q^2=0}$$

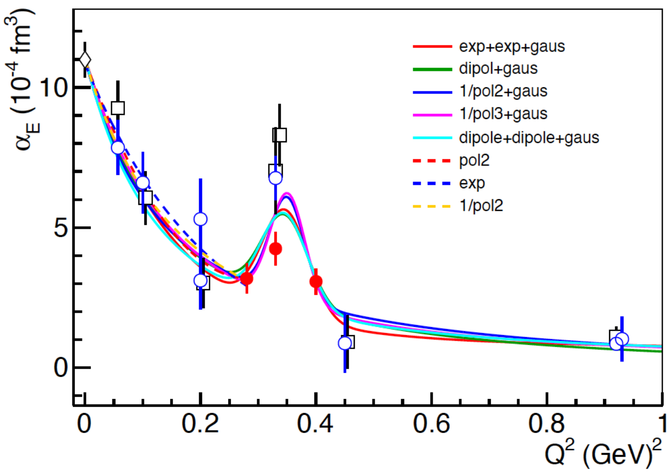

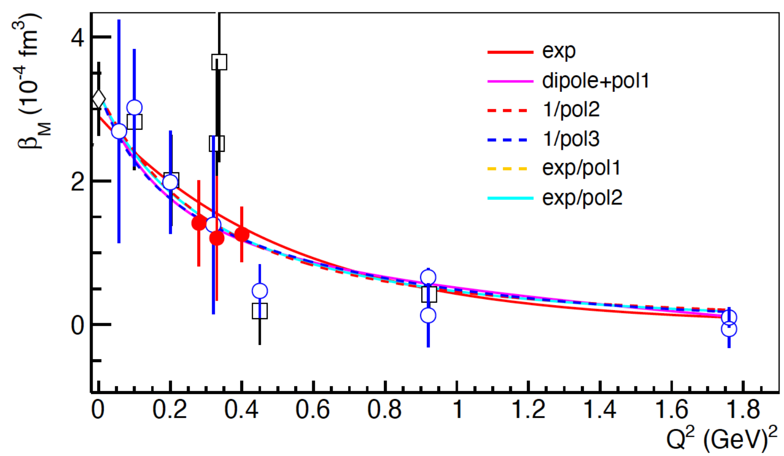

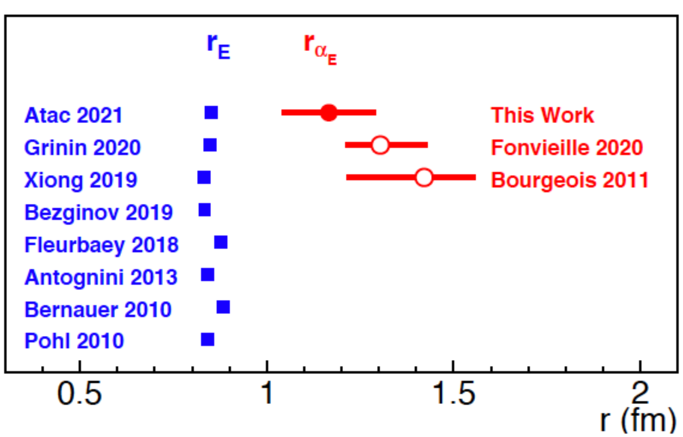

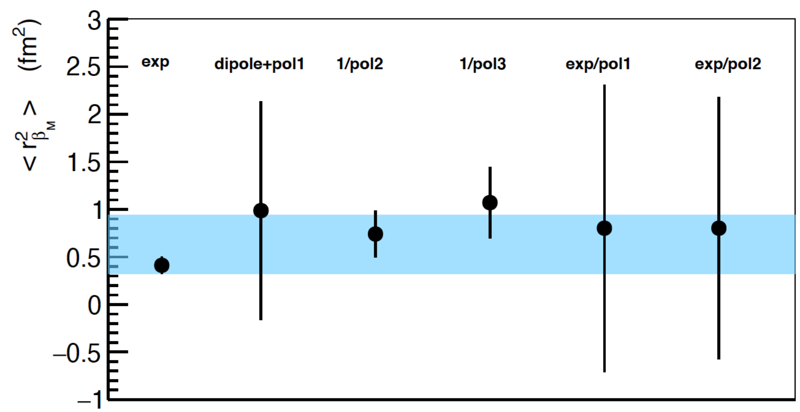

$$\langle r^2_{\alpha_E} \rangle = 1.36 \pm 0.29 \text{ fm}^2$$

$$\langle r^2_{\beta_M} \rangle = 0.63 \pm 0.31 \text{ fm}^2$$

Moving Forward

VCS-II Experimental Setup

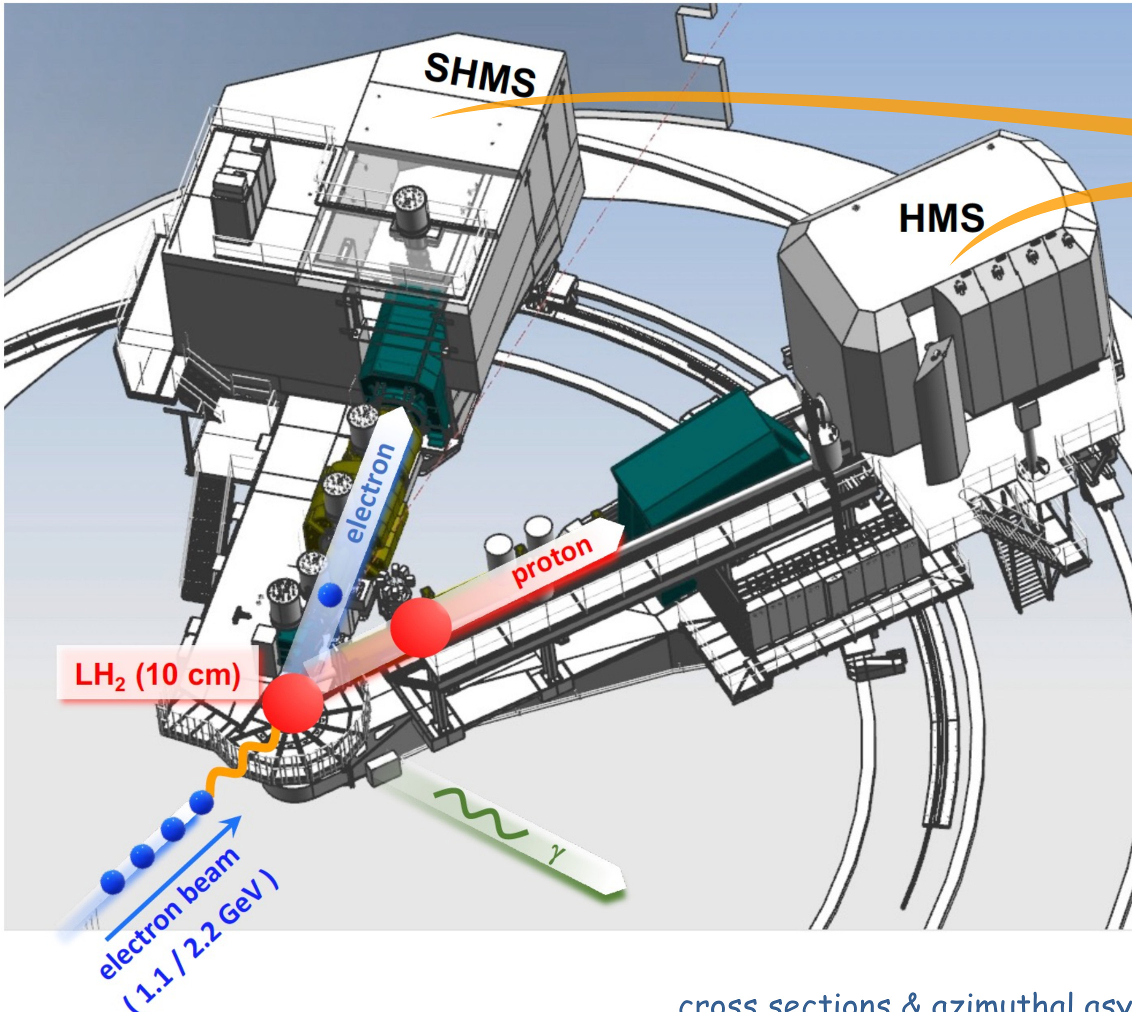

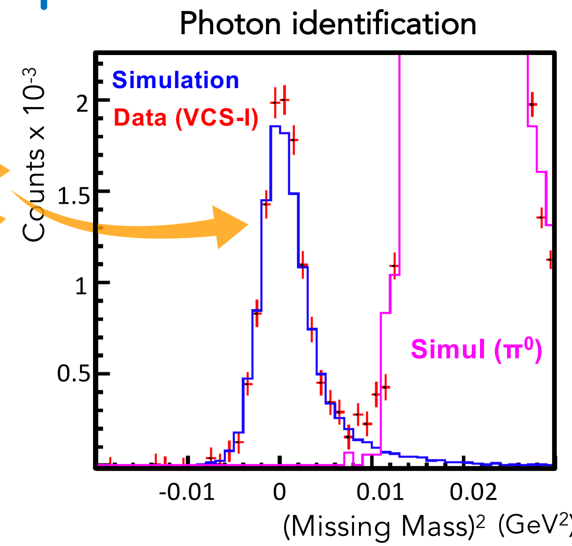

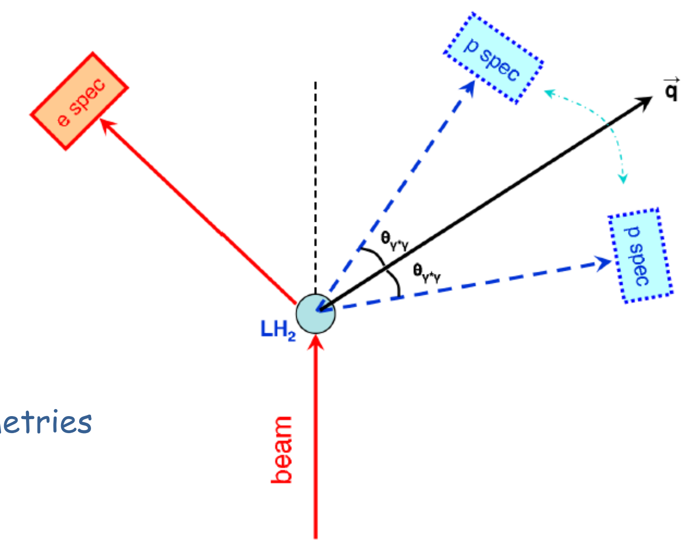

cross sections & azimuthal asymmetries

$$A_{(\phi_{\gamma^*\gamma}=0,\pi)} = \frac{\sigma_{\phi_{\gamma^*\gamma}=0} - \sigma_{\phi_{\gamma^*\gamma}=180}}{\sigma_{\phi_{\gamma^*\gamma}=0} + \sigma_{\phi_{\gamma^*\gamma}=180}}$$

suppression of systematic uncertainties

Extra handle to spectrometer momentum calibration

Hall C: SHMS, HMS

E= 1.1 GeV (lowest Q^2)
E=2.2 GeV (all other settings)

Liquid hydrogen 10 cm

VCS-II Experimental Setup

Selection of kinematics

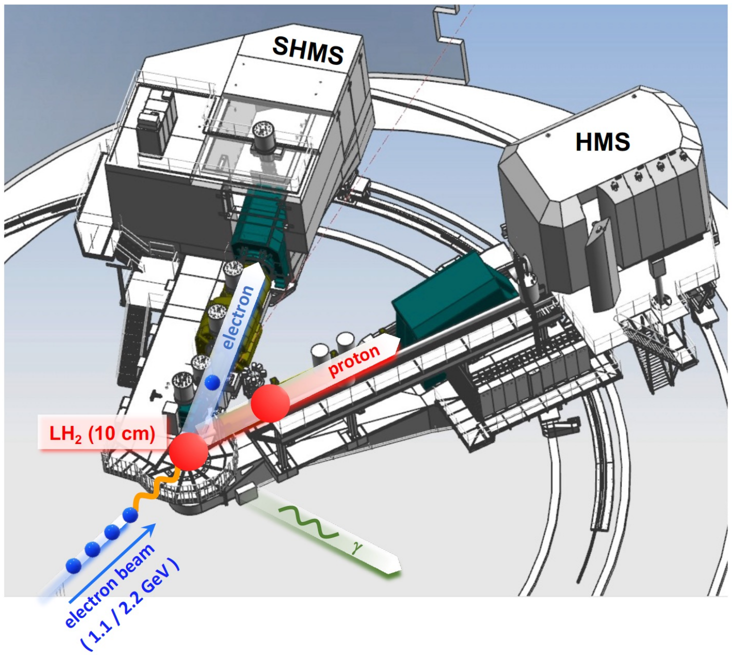

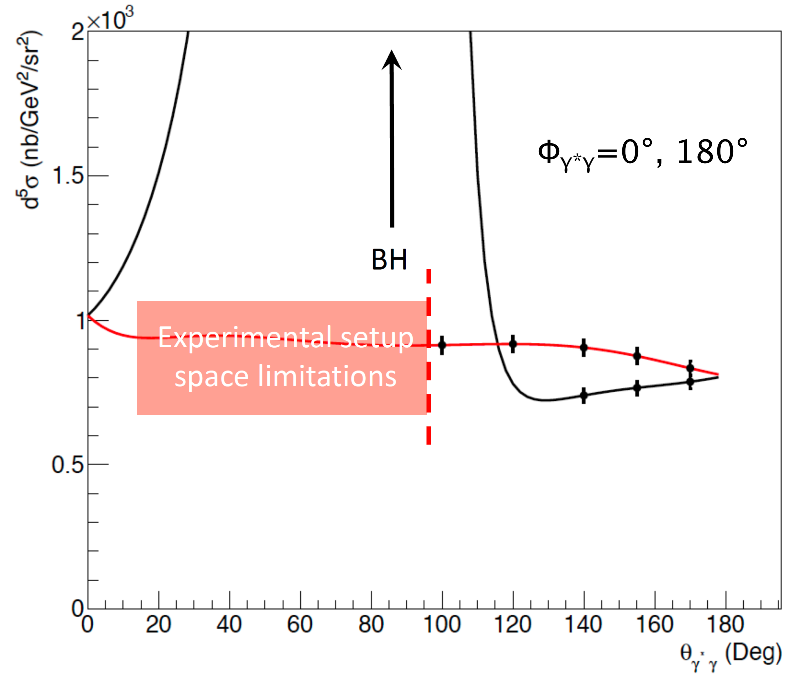

Targeted measurements to fully exploit the sensitivity to the GPs

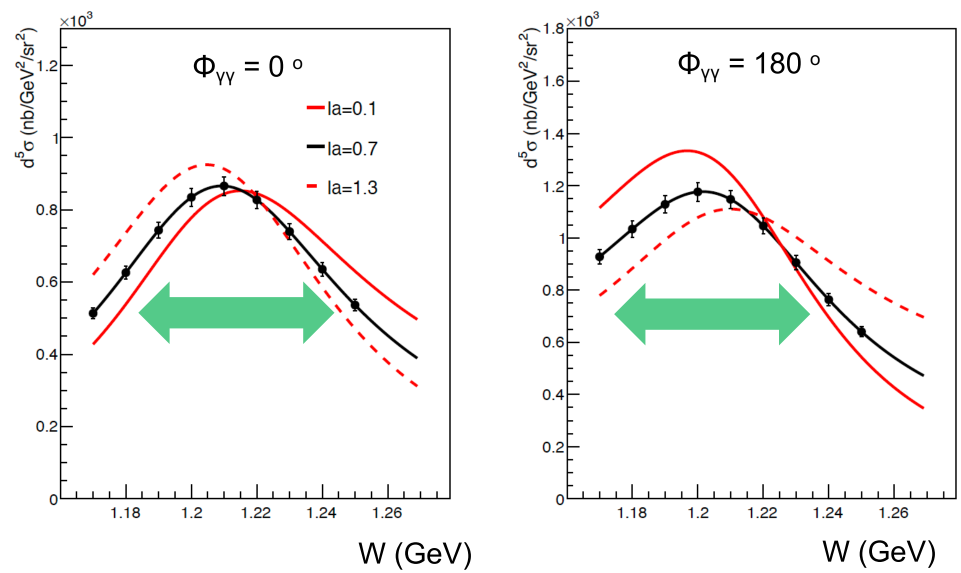

Kinematics

Q^2 spans 0.05 GeV^2 to 0.5 GeV^2

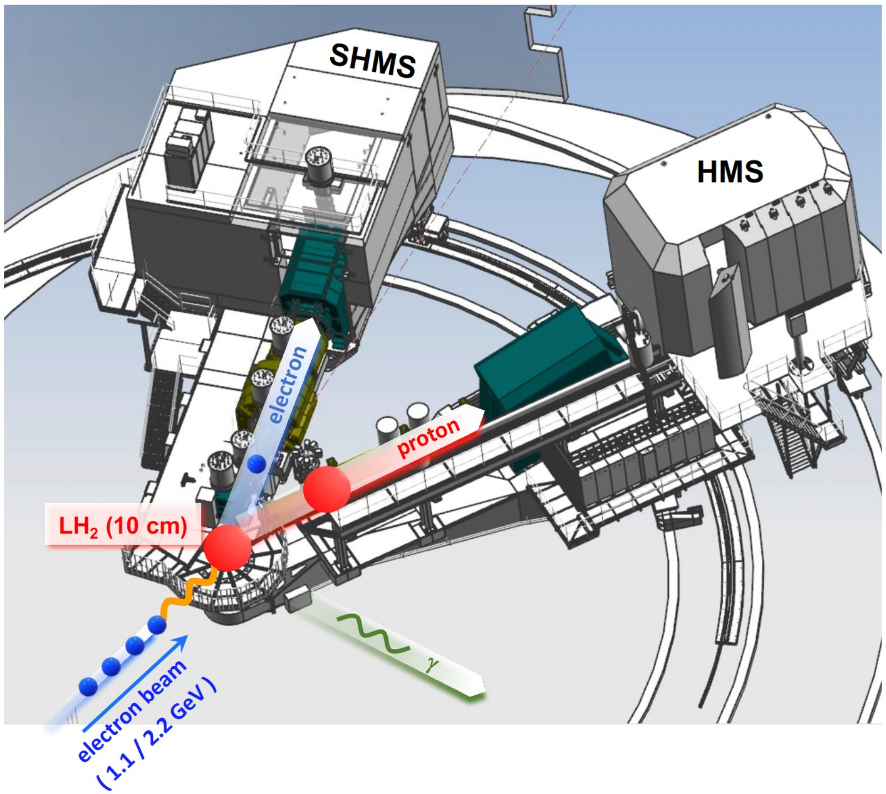

Production (E_o = 1.1 GeV) :	6 days
Production (E_o = 2.2 GeV) :	53 days
Studies (optics/dummy/calibrations) :	3 days

Total: 62 days

Kinematic Group	Kinematic Setting	$\theta_{\gamma^*\gamma}$°	θ_e°	$P_e'(MeV/c)$	θ_p°	$P_p'(MeV/c)$	I (μA)	beam time (days)
GI	Kin I	110	14.3	736.3	54.45	493.93	15	1.00
	Kin II	133	14.3	736.3	44.93	556.10	15	1.00
	Kin IIIa	147	14.3	736.3	11.26	583.05	15	1.00
	Kin IIIb	147	14.3	736.3	39.06	583.05	15	1.00
	Kin IVa	160	14.3	736.3	16.73	599.95	15	1.00
	Kin IVb	160	14.3	736.3	33.59	599.95	15	1.00
GII	Kin I	115	11.22	1783.0	15.33	615.69	10	1.50
	Kin IIa	125	11.22	1783.0	56.54	647.85	10	2.50
	Kin IIb	125	11.22	1783.0	18.60	647.85	10	1.50
	Kin IIIa	145	11.22	1783.0	49.77	697.99	10	1.50
	Kin IIIb	145	11.22	1783.0	25.37	697.99	10	1.00
	Kin IVa	165	11.22	1783.0	42.82	726.87	10	1.00
	Kin IVb	165	11.22	1783.0	32.32	726.87	10	1.00
GIII	Kin I	115	14.73	1729.7	20.58	706.89	30	1.75
	Kin IIa	130	14.73	1729.7	54.89	758.24	30	2.00
	Kin IIb	130	14.73	1729.7	24.78	758.24	30	1.75
	Kin IIIa	150	14.73	1729.7	48.99	808.24	30	1.75
	Kin IIIb	150	14.73	1729.7	30.68	808.24	30	1.75
	Kin IVa	170	14.73	1729.7	42.90	834.12	30	1.00
	Kin IVb	170	14.73	1729.7	36.76	834.12	30	1.00
GIV	Kin I	100	16.32	1749.3	23.83	664.52	35	1.75
	Kin II	120	16.32	1749.3	28.01	738.39	50	1.25
	Kin IIIa	140	16.32	1749.3	32.84	795.37	70	1.00
	Kin IIIb	140	16.32	1749.3	53.80	795.37	70	2.00
	Kin IVa	155	16.32	1749.3	36.69	824.46	70	1.50
	Kin IVb	155	16.32	1749.3	49.95	824.46	70	2.50
	Kin Va	170	16.32	1749.3	40.66	840.48	70	1.00
	Kin Vb	170	16.32	1749.3	45.99	840.48	70	1.00
GV	Kin I	100	17.72	1676.41	19.75	723.69	35	2.00
	Kin II	120	17.72	1676.41	24.25	808.93	50	1.50
	Kin IIIa	140	17.72	1676.41	29.34	874.74	70	1.50
	Kin IIIb	140	17.72	1676.41	51.12	874.74	70	2.00
	Kin IVa	155	17.72	1676.41	33.36	908.37	70	2.00
	Kin IVb	155	17.72	1676.41	47.10	908.37	70	2.00
	Kin Va	170	17.72	1676.41	37.47	926.91	70	1.00
	Kin Vb	170	17.72	1676.41	42.99	926.91	70	1.00
GVI	Kin I	120	20.45	1623.1	25.31	886.59	75	1.00
	Kin IIa	140	20.45	1623.1	29.91	956.82	75	1.00
	Kin IIb	140	20.45	1623.1	49.81	956.82	75	1.50
	Kin IIIa	155	20.45	1623.1	33.58	992.83	75	1.50
	Kin IIIb	155	20.45	1623.1	46.14	992.83	75	2.00

Projected Cross sections

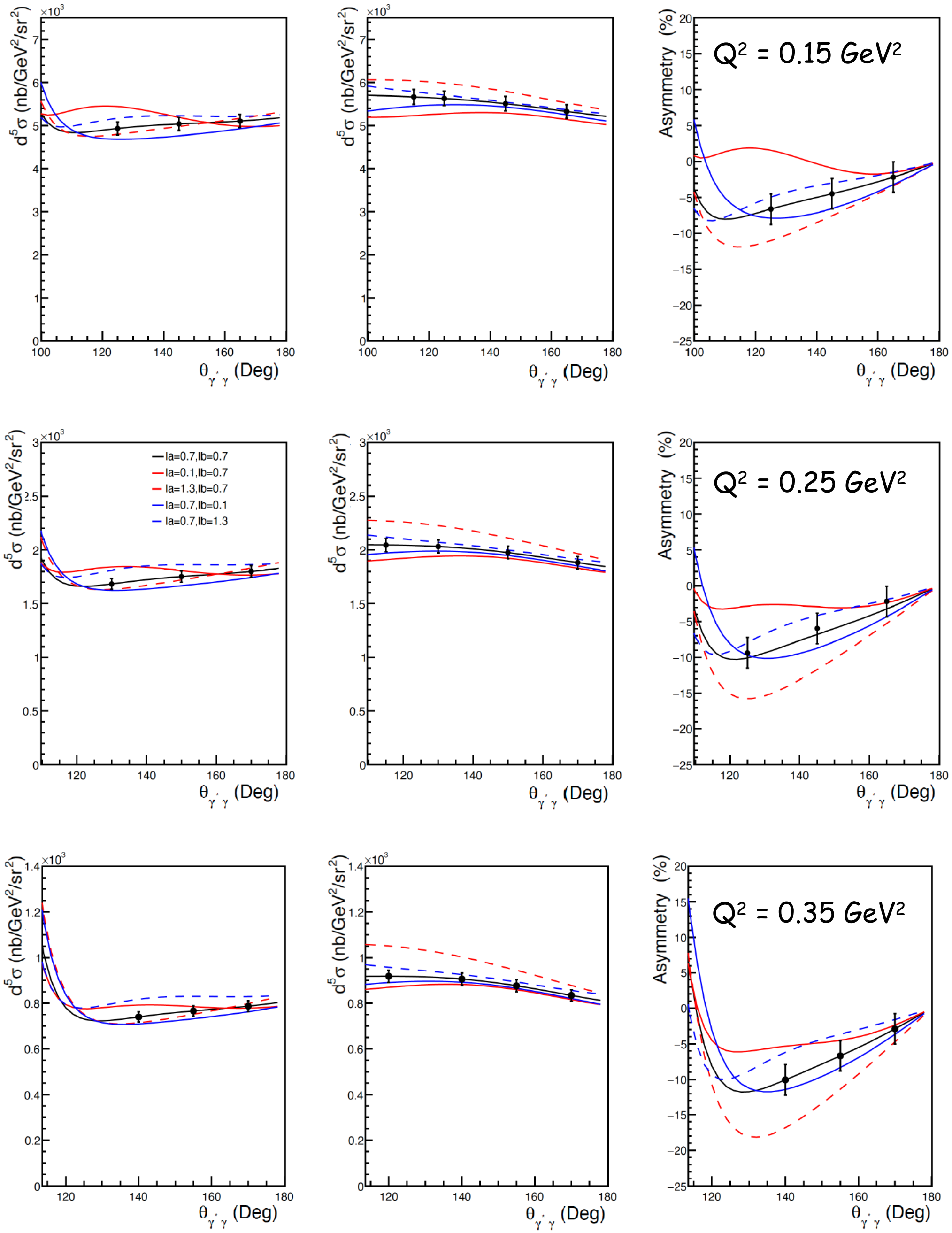

VCS-II Projected

δ(stat) = 1% - 2%

δ(syst) = 3.5% - 4%

VCS-II Projected Measurements

High precision measurements
combined with a fine mapping in Q^2

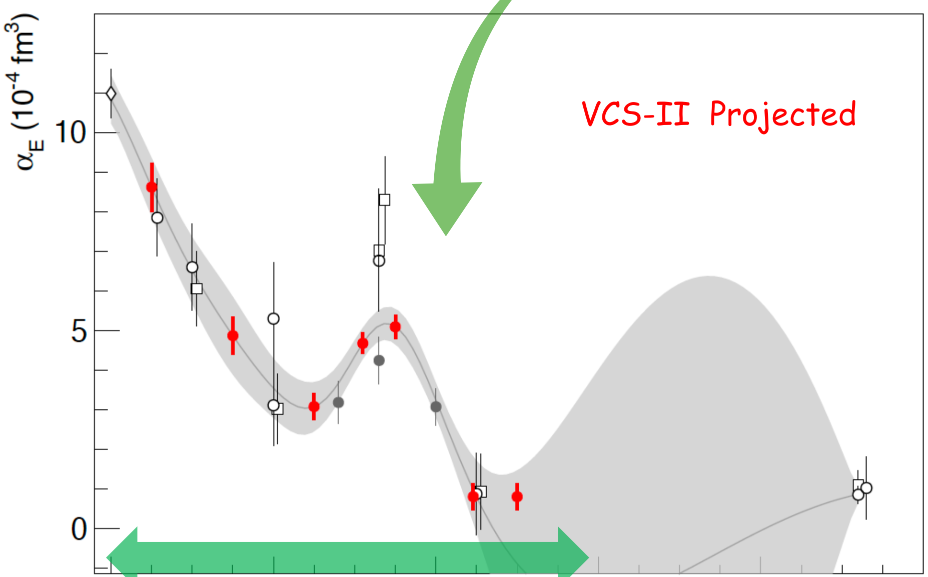

systematically consistent
measurements throughout Q^2

Targeted measurements to fully
exploit the sensitivity to the GPs

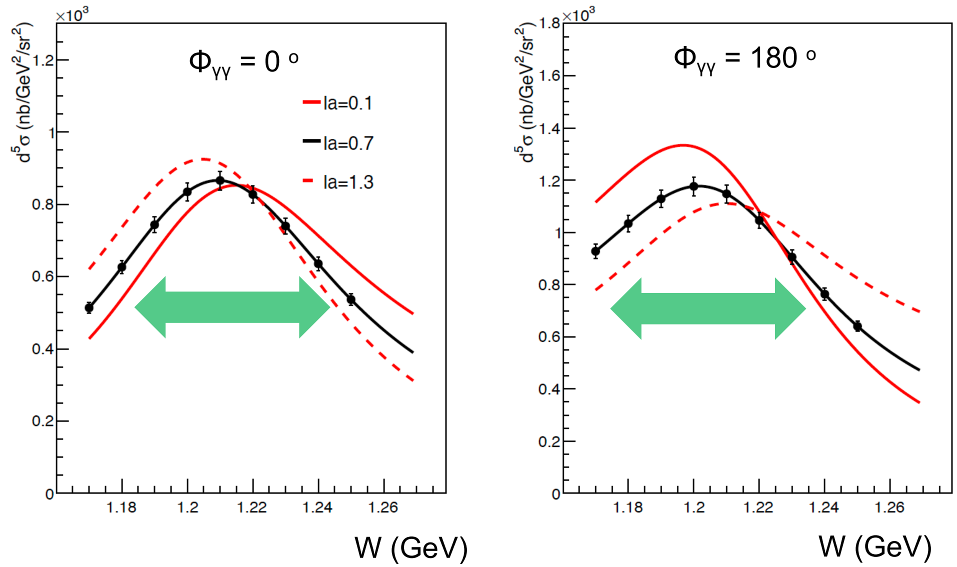

Improve upon β_M :

Pin down the competing
para/dia-magnetic contributions
in the nucleon

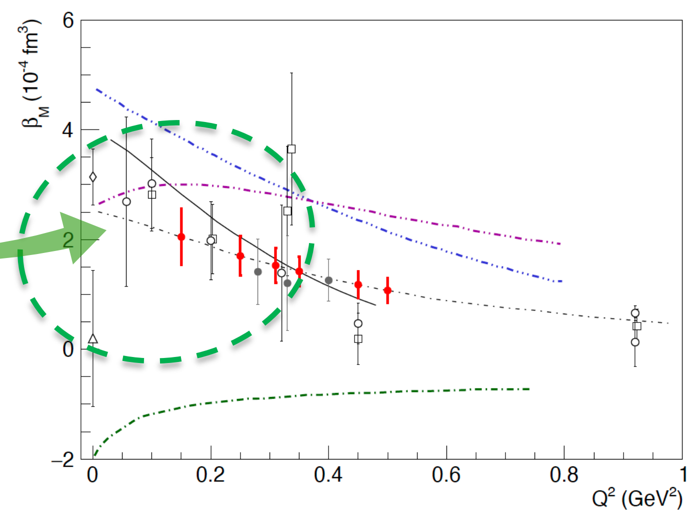

Other prospects: Measuring with positrons or with polarized e^- beam

Positrons allow for an <u>independent path</u> to access experimentally the GPs

Eur. Phys. J. A 57 (2021) 11, 316

Virtual Compton scattering at low energies with a positron beam

Barbara Pasquini[a,1,2], **Marc Vanderhaeghen**[b,3]

[1]Dipartimento di Fisica, Università degli Studi di Pavia, 27100 Pavia, Italy
[2]Istituto Nazionale di Fisica Nucleare, Sezione di Pavia, 27100 Pavia, Italy
[3]Institut für Kernphysik and PRISMA+ Cluster of Excellence, Johannes Gutenberg Universität, D-55099 Mainz, Germany

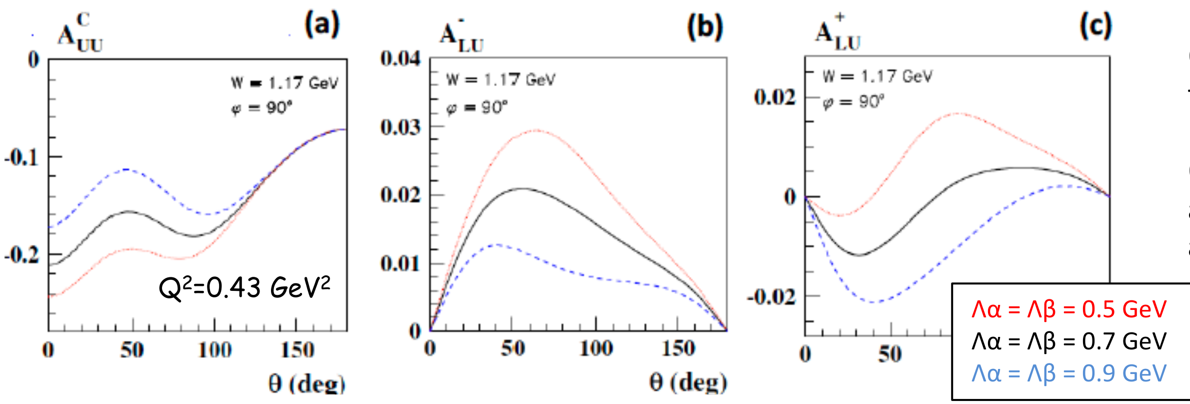

(a): The beam-charge asymmetry as a function of the photon scattering angle at Q2 = 0.43 GeV 2.

(b) & (c): The electron and positron beam-spin asymmetry as a function of the photon scattering angle for out-of-plane kinematics.

Unpolarized beam charge asymmetry (BCA) : $$A^C_{UU} = \frac{(d\sigma^+_+ + d\sigma^+_-) - (d\sigma^-_+ + d\sigma^-_-)}{d\sigma^+_+ + d\sigma^+_- + d\sigma^-_+ + d\sigma^-_-}$$

Lepton beam spin asymmetry (BSA) : $$A^e_{LU} = \frac{d\sigma^e_+ - d\sigma^e_-}{d\sigma^e_+ + d\sigma^e_-}$$

BCA

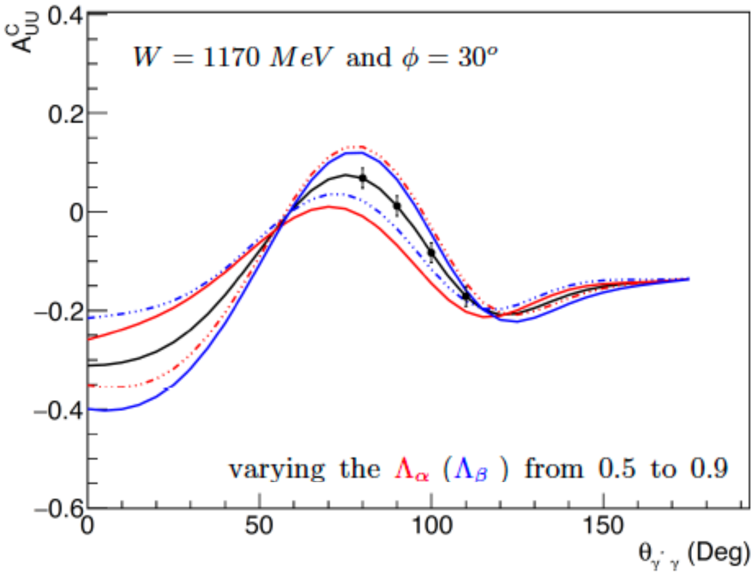

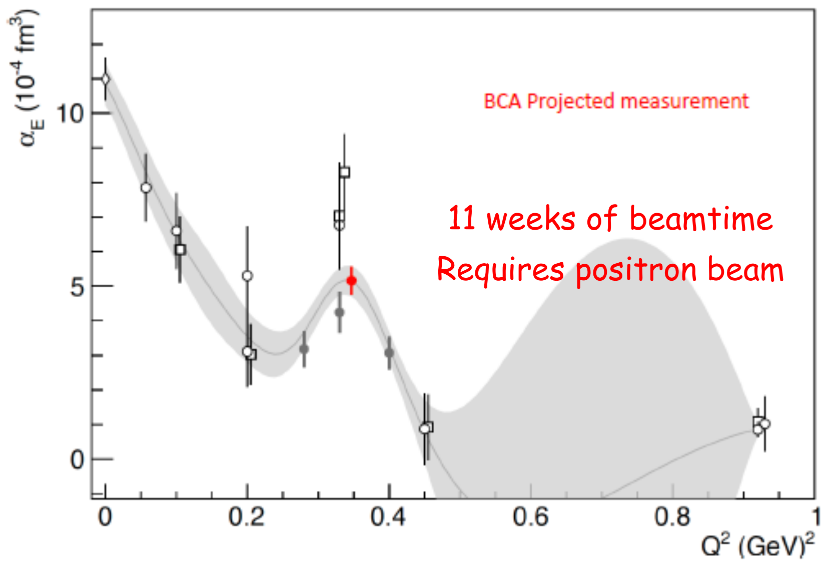

Hall C (SHMS / HMS)

- e^- : ~ 1 week of beamtime @ 50 μA
- and
- e^+ : ~ 10 weeks of beamtime @ 5 μA

BSA

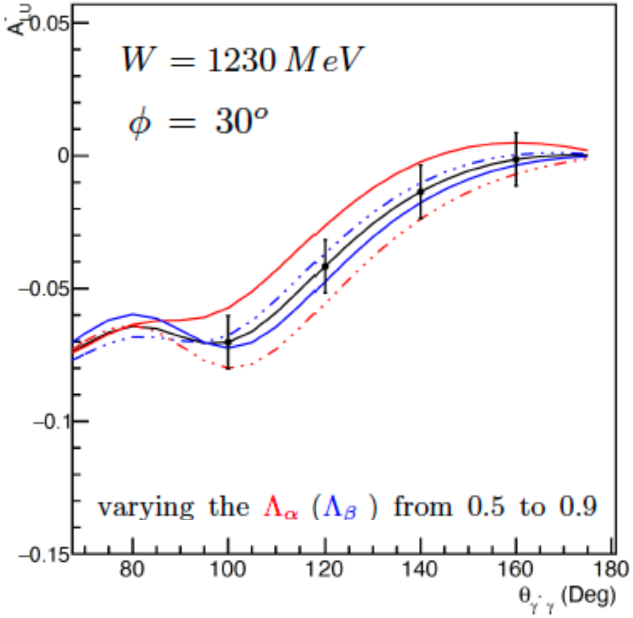

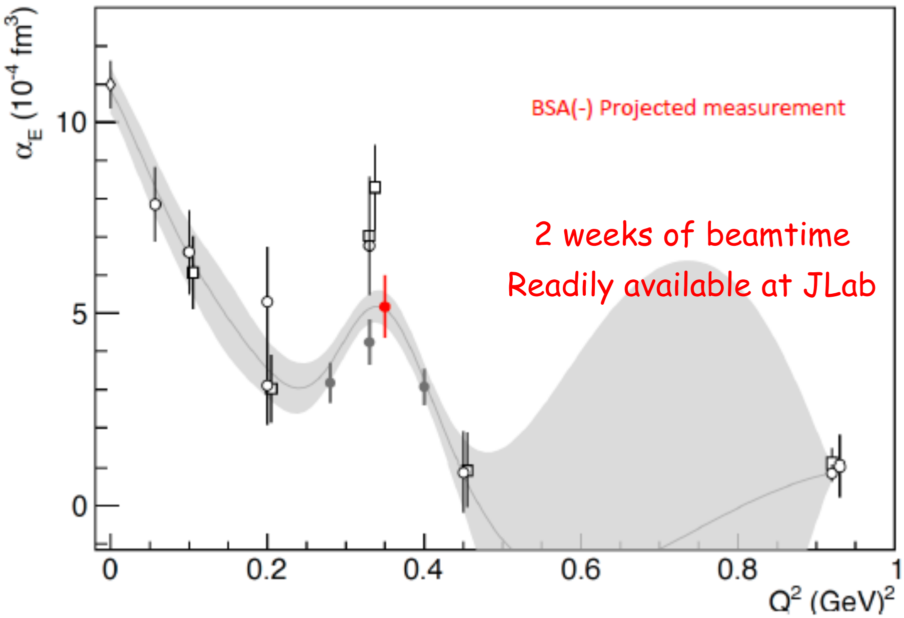

Hall C (SHMS / HMS)

- e^- (pol. 85% @ 70 μA) : ~ 2 weeks of beamtime

  or

- e^+ (pol. 60% @ 50 nA) : ~ 3 orders of magnitude more beamtime

Measurement of the Generalized Polarizabilities of the Proton with positron and polarized electron beams

Letter of Intent to Jefferson Lab PAC-51

Summary

Progress in the study of fundamental system properties
that characterize the proton's response to an EM field

Insight to spatial deformation of the nucleon densities under an applied EM field, interplay of para/dia-magnetic mechanisms in the proton, polarizability radii, …

Electric GP:
- possibility for a non-trivial (non-monotonic) behavior in $\alpha_E(Q^2)$ (albeit with a smaller magnitude than originally suggested)

  or

- at minimum: strong tension between world data

Strong constraints to theoretical predictions (and we can improve further)

High precision benchmark data for theory & upcoming LQCD calculations

Future measurements:

- Pinn down with precision the shape of the α_E structure (if it exists) - important input for the theory
- Measure via a different channel (positrons)

Thank you!

BACK UP

Static Polarizabilities

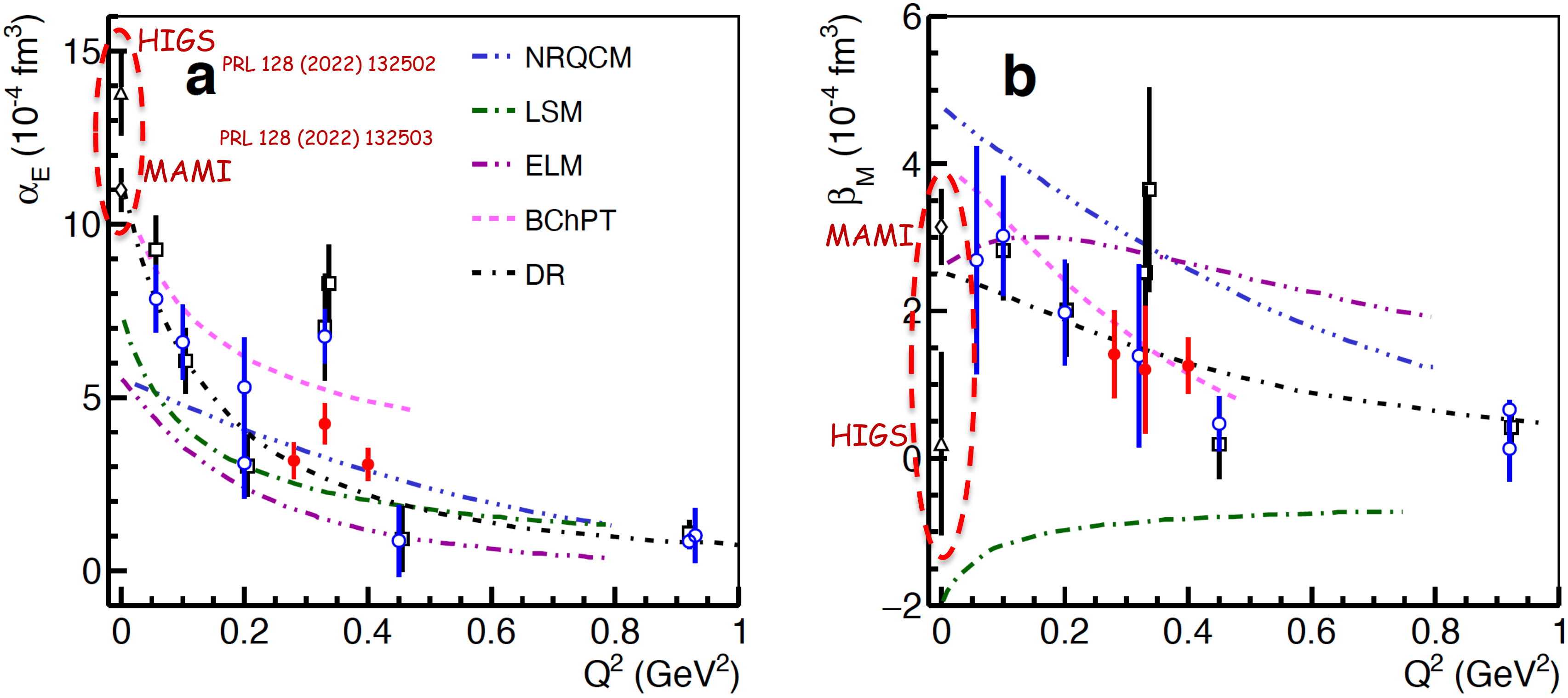

Static Polarizabilities

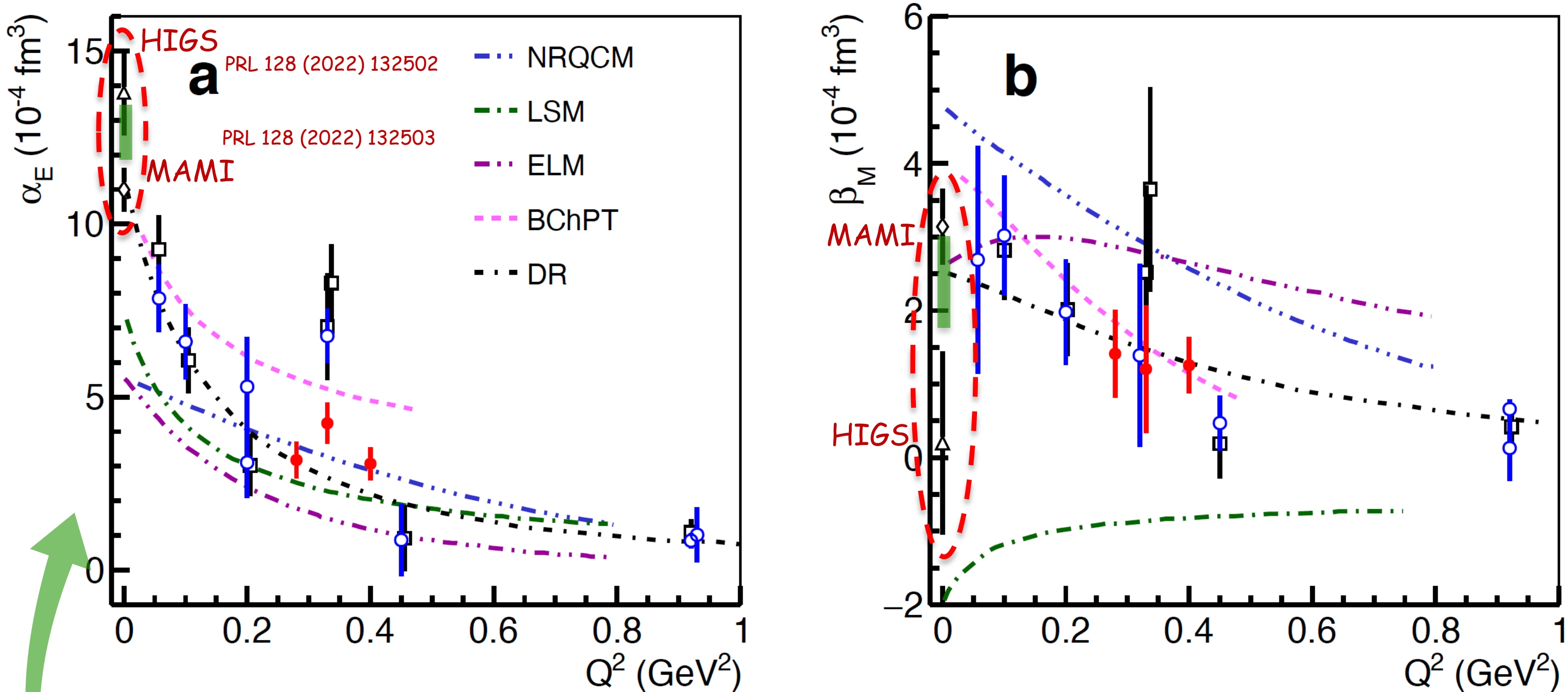

PHYSICAL REVIEW LETTERS **129**, 102501 (2022)

First Concurrent Extraction of the Leading-Order Scalar and Spin Proton Polarizabilities

E. Mornacchi,[1,*] S. Rodini,[2] B. Pasquini,[3,4] and P. Pedroni[4]

[1]*Institut für Kernphysik, Johannes Gutenberg-Universität Mainz, D-55099 Mainz, Germany*
[2]*Institut für Theoretische Physik, Universität Regensburg, D-93040 Regensburg, Germany*
[3]*Dipartimento di Fisica, Università degli Studi di Pavia, I-27100 Pavia, Italy*
[4]*INFN Sezione di Pavia, I-27100 Pavia, Italy*

(Received 3 May 2022; revised 11 July 2022; accepted 2 August 2022; published 31 August 2022)

We performed the first simultaneous extraction of the six leading-order proton polarizabilities. We reached this milestone thanks to both new high-quality experimental data and an innovative bootstrap-based fitting method. These new results provide a self-consistent and fundamental benchmark for all future theoretical and experimental polarizability estimates.

$$\alpha_{E1} = [12.7 \pm 0.8(\text{fit}) \pm 0.1(\text{model})] \times 10^{-4}\ \text{fm}^3,$$
$$\beta_{M1} = [2.4 \pm 0.6(\text{fit}) \pm 0.1(\text{model})] \times 10^{-4}\ \text{fm}^3,$$
$$\gamma_{E1E1} = [-3.0 \pm 0.6(\text{fit}) \pm 0.4(\text{model})] \times 10^{-4}\ \text{fm}^4,$$
$$\gamma_{M1M1} = [3.7 \pm 0.5(\text{fit}) \pm 0.1(\text{model})] \times 10^{-4}\ \text{fm}^4,$$
$$\gamma_{E1M2} = [-1.2 \pm 1.0(\text{fit}) \pm 0.3(\text{model})] \times 10^{-4}\ \text{fm}^4,$$
$$\gamma_{M1E2} = [2.0 \pm 0.7(\text{fit}) \pm 0.4(\text{model})] \times 10^{-4}\ \text{fm}^4,$$

Blue bins = where the higher-order estimator is < 3%
(LEX truncation « valid »)

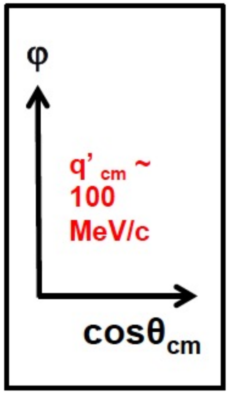

VCS expt :	Bates	MAMI	MAMI	MAMI	MAMI	JLab
Q2 (GeV2) =	0.06	0.10	0.20	0.33	0.45	0.92

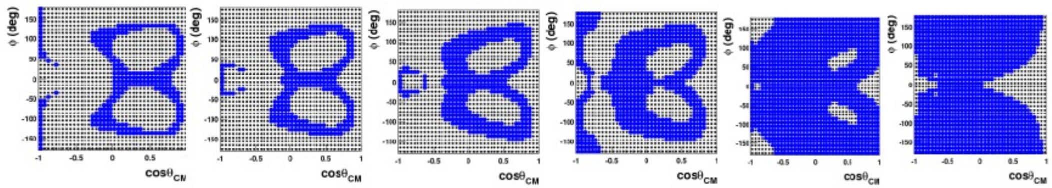

New « vcsq2 » data:

- OOP kinematics (to access the blue region)

-LEX Fit done with bin selection at Q^2 = 0.1 and 0.2 GeV^2.

- was found not necessary at Q^2 = 0.45 GeV^2.

In-plane

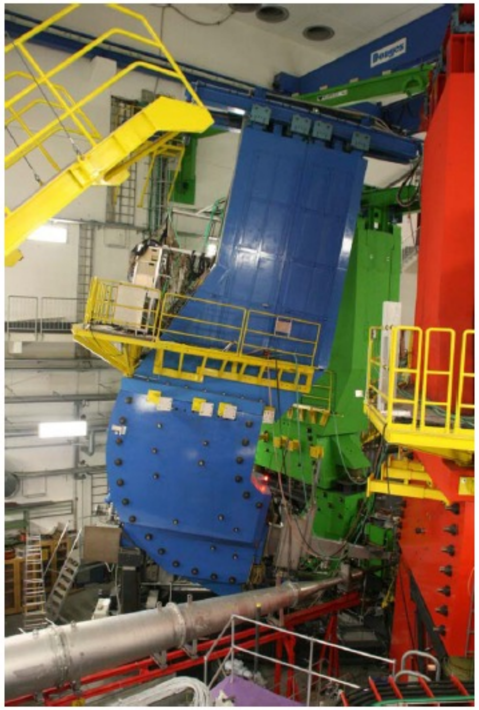

8.5 deg OOP

(material from H. Fonvieille)

A1/1-09 @ MAMI

~ 1.0 GeV beam

Q^2 = 0.1 $(GeV/c)^2$, 0.2 $(GeV/c)^2$, and 0.45 $(GeV/c)^2$

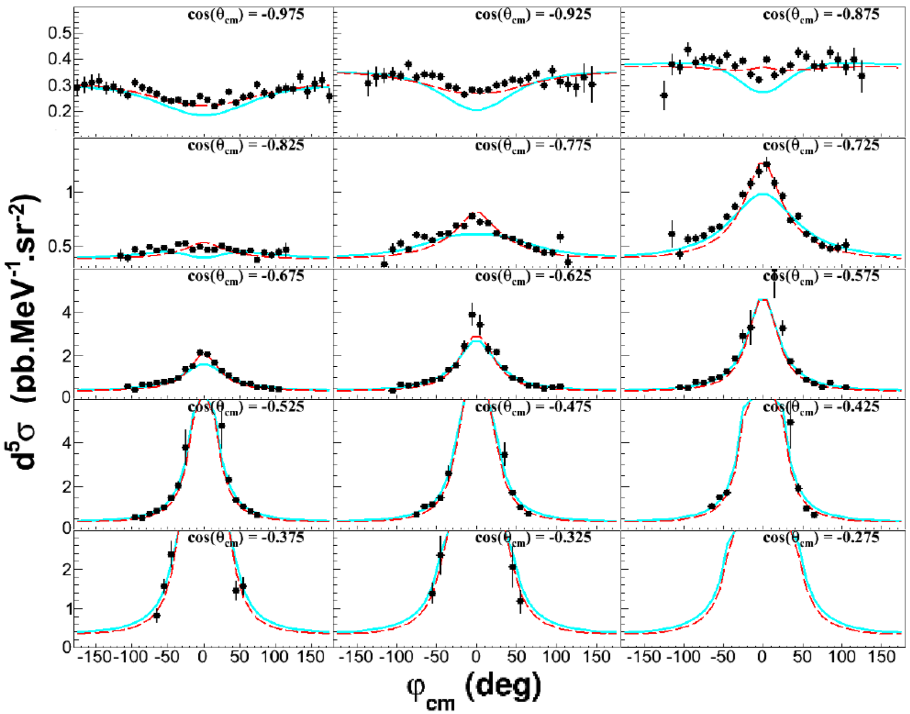

Figure 5.8: Setting INP: measured $ep \to ep\gamma$ cross section at fixed q'_{cm} = 112.5 MeV/c with respect to φ_{cm} for all the $cos(\theta_{cm})$-bins. The curves follow the convention of figure 5.6.

Figure from PhD thesis of L. Correa, Mainz / Cl. Ferrand

BH+B ---

Polarizability effect ---

GP effect typically 5% – 15% of the cross section

Polarizability fits:

DR fit:
DR calculation includes full dependency in q'_{cm}

LEX fit:
truncated in q'cm. Suppress contribution from higher order terms

Virtual Compton Scattering

Phys. Rev C 86, 015210 (2012)

Phys. Rev Lett. 93, 122001 (2004)

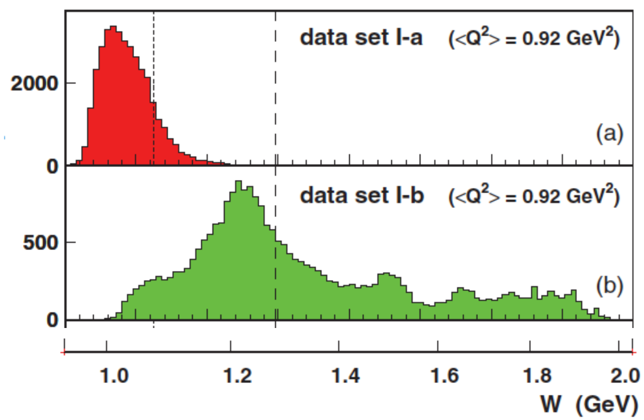

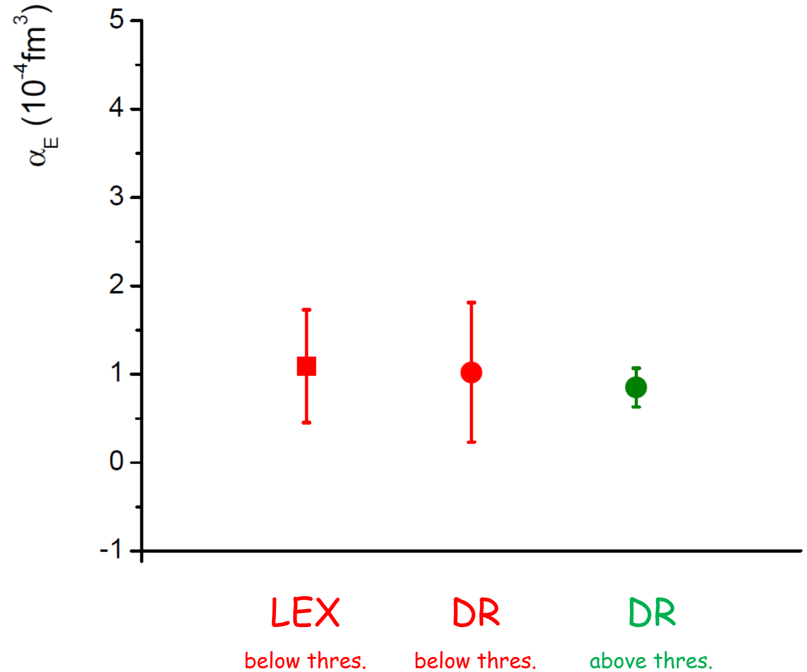

Sensitivity to the GPs grows as we measure above pion threshold